SPATIO-TEMPORAL WATER RESOURCE RESPONSES TO LAND USE LAND COVER CHANGE IN SEMI-ARID UPPER TEKEZE BASIN, NORTHERN ETHIOPIA

PhD Research Proposal

Mewcha Amha Gebremedhin

Committee members:

Dr. ir. M.W. Lubczynski	promoter	University of Twente, ITC
Dr. B.H.P. Maathuis	co-promoter	University of Twente, ITC
Dr. Daniel Teka	co-promoter	Mekelle University, I-GEOS

ITC
UNIVERSITY OF TWENTE.

Abstract

Water shortage remains a prevalent problem in the semi-arid Upper Tekeze Basin (UTB) due to the short duration of the rainy season and high rainfall variability. This has been resulted in recurrent droughts and the groundwater is also affected, especially in the dry season, with many wells getting drier. The Growth and Transformation Plan (GTP) of Ethiopia envisages more intensive agricultural practices and land use land cover (LULC) changes. The future LULC can exacerbate the water shortage by affecting the complex water fluxes in the surface and groundwater domains. This requires in depth investigations of the spatio-temporal surface-groundwater interactions and groundwater resources changes. This can be realized through the application of an integrated hydrological models (IHM). However, the poor coverage of ground-based hydro-meteorological gauging stations challenged application of the IHM. Therefore, this study proposes research approach consisting of three main objectives to address the aforementioned problems in the UTB. Firstly, relatively high resolution satellite derived rainfall and potential evapotranspiration estimations will be validated. The satellite based products will be merged with in-situ observations to improve their quality and these will be used to address the spatio-temporal input for the IHM. Secondly, an IHM will be conceptualized and calibrated to quantify the surface-groundwater interactions and groundwater resources in a spatio-temporal manner. Thirdly, LULC change will be predicted and afterwards used as constrain in the IHM to predict future water resources changes. This study is part Ethiopian Education Network to Support Agricultural Transformation (EENSAT) project and it will contribute to the objective of integrating geo-spatial data and earth observation techniques for water resource applications. The output of this study will contribute to sustainable water resource management and as a pilot study that can be followed in other Basins in Ethiopia.

Keyword: satellite derived rainfall and potential evapotranspiration, surface-groundwater interaction, integrated hydrological modeling, land use land cover change prediction, Upper Tekeze Basin, Ethiopia

Table of Contents

List of figures

List of tables

List of abbreviations

ARC	Africa Rainfall Climatology
ARC2	African Rainfall Climatology version 2
BAU	Business as Usual
CHIRPS	Climate Hazards Group InfraRed Precipitation with Station
CMORPH	Climate Prediction Center's morphing technique
DEM	Digital Elevation Model
EENSAT	Ethiopian Educational Network to Support Agricultural Transformation
FCWP	Forest Conservation and Water Protection
GSFLOW	Groundwater and Surface-water FLOW
GTP	Growth and Transformation Plan
GWR	Geographical Weighted Regression
LULC	Land Use Land Cover
MPEG	Multi-Sensor Precipitation Estimate-Geostationary
NMA	National Meteorological Agency
PERSIANN	Precipitation Estimation from Remotely Sensed Information using Artificial Neural Networks
RFE	African rainfall estimation algorithm
SRTM	Shuttle Radar Topographic Mission
TAMSAT	Tropical Applications of Meteorology using Satellite data and and ground-based observations
TRMM	Tropical Rainfall Measuring Mission
UTB	Upper Tekeze Basin

1. Introduction

1.1. background

Nowadays, water availability is declining with increasing population growth and this may be seriously affect the economic growth of the glob (Zhou et al., 2015; Moral et al., 2016; Distefano & Kelly, 2017; Yihdego & Khalil, 2017). Human-based interventions are the main factors affecting water resources availability and distribution (Haddeland et al., 2014). Land Use Land Cover (LULC) change is one of the human manifested factors altering the quantity and distribution of both surface and ground water resources. LULC change is a global challenge because it drives various environmental changes at all spatial and temporal scales (Bosmans et al., 2017; Gashaw et al., 2017). Globally, the impact of LULC on water resources is larger compare to impacts by climate change and water abstraction (Rost et al., 2008). As a result, many studies have been conducted on LULC impact on water resources at different scales, particularly more rely on surface hydrology (eg. Liu et al., 2004; Öztürk et al., 2013; Gyamfi et al., 2016; Taye et al., 2014; Welde & Gebremariam, 2017). The impact of LULC change on hydrological response differs with different LULC. For example, a study by Woldesenbet et al.(2017a) showed that runoff increases and groundwater declines as forest cover decreases and arable land increases. Deforestation and agriculture increment resulted in decreasing evapotranspiration and increase in total runoff (Mao & Cherkauer, 2009). LULC significantly affects the infiltration, interception and evapotranspiration of hydrological processes (Mohan et al., 2018; García-Leoz et al., 2018; Brasil et al., 2018; Teklay et al., 2019). These all indicate that LULC change affects the complex water fluxes in the surface and subsurface domains. Moreover, LULC could result in an increase of water scarcity and thus contribute to a deterioration of living conditions particularly in regions where water availability is limited (Wagner et al., 2013).

Arid and semi-arid regions with water scarce resources in developing countries are facing drastic LULC changes as a result of rapidly increasing human population and socio-economic developments (Kumar et al., 2018). Therefore, understanding and quantifying the water fluxes under LULC change is important for sustainable water resource management. Quantifying the water availability is dependent on how rainfall over a given area is distributed into various hydrologic processes and how proportions of these processes are related to LULC (Sajikumar & Remya, 2015). However, it is difficult to analyze the hydrologic processes simultaneously without an integrated surface-groundwater framework as they covary temporally and spatially and are correlated with each other (Huntington and Niswonger, 2012).

Water resources quantification needs accurate input data for adequate descriptions of spatial and temporal water distribution. However, the scarcity of in-situ observations is common, particularly in developing countries. Rainfall is among the key variables where hydrological studies rely on its quality to produce representative modeling output. In-situ observations have also a major limitation to describe the spatial representation of rainfall required by hydrological modeling applications (Nerini et al., 2015). With the advancement of technologies, remote sensing derived rainfall products are a suitable alternative to in-situ measurements (Thiemig et al., 2013; Seyyedi et al., 2014; Rahmawati and Lubczynski, 2017; Retalis et al., 2017; Zambrano-Bigiarini et al., 2017; Ayehu et al., 2018; dos Reis et al., 2017; Lekula et al., 2018). Satellite derived rainfall products are a potential source for forcing inputs in driving hydrological models especially in sparse or ungauged complex terrain (Alazzy et al., 2017). The representativeness of satellite based rainfall is more relevant when they are integrated with the in-situ observed rainfalls (Fang et al., 2013).Potential evapotranspiration is another important component of hydrological driving force for water resources assessment; however finding spatially representative climatic variables constrain its application in many regions (Oudin et al , 2010; Lang et al., 2017). Similar to the rainfall, satellite based potential evapotranspiration estimations are also good alternative source at different spatio-temporal scales (Kim & Hogue, 2008; Ndou et al., 2017; Zhang et al., 2018). These products are particularly important in arid and semi-arid areas where the required in-situ input to compute potential evapotranspiration are scarce. Therefore, satellite derived hydrological driving are heavily suitable for water resource applications spatially and temporally particularly as input to hydrological modellings.

Water balance models have been carried out in water resources research applications at different spatial and temporal scales since 19^{th} century (Xu and Singh, 2004). However, the interaction between groundwater and surface components of the hydrologic system has been neglected or simplified by these models (Liang, 2003; Yeh and Eltahir, 2005; Niu et al., 2014). Nowadays, the integration of groundwater processes in existing land-surface models is becoming an active field of research because understanding the basic principles of interactions between surface and groundwater is key input for effective management of water resources (Hassan et al., 2014; Feng et al., 2018; Sridhar et al., 2018). Such interaction can be realized using integrated hydrological models since they are useful tools to analyze the complex water resources problems at reasonable spatial and temporal details (Markstrom et al., 2008b; Tian et al., 2018).

The spatio-temporal variability of water resources in Ethiopia is characterized by rainfall variability (Melesse et al., 2013). The spatio-temporal variability of the surface water of the country follows the pattern of the rainfall variability. The occurrence of groundwater also varies with influence of geophysical and climatic conditions (Alemayehu, 2006). The surface-groundwater interactions on such geologically and topographically varied area can better characterized by integrated hydrological models. However, some studies conducted around UTB are only focusing on surface runoff (Eg. Tesfagiorgis et al., 2011; Welde & Gebremariam, 2017) or groundwater recharge resources as separate entities. For example, Haregeweyn et al. (2015) estimated spatially distributed average annual evapotranspiration, surface runoff, and groundwater recharge using WetSpa model in Gilgel Tekeze. The results from this study could not show the spatio-temporal variation of water balances. Tesfagiorgis et al. (2011) evaluated groundwater resources in the Geba Basin using MODFLOW groundwater model in a PMWIN environment. The authors used mean annual recharge from 2001 as input to the model with no spatial variability. Based on results from such studies, it is difficult to conclude on the groundwater resource distribution under complex topography and hydro-geologically variable terrain. Gebreyohannes et al (2017) also used similar approach to Tesfagiorgis et al. (2011) to model regional groundwater flow in Giba Basin under multiple layers and their result interprets only the inflow and outflow from recharge as water balance components. Overall, none of them used integrated modelling approach that accounts complicated non-linear processes such as groundwater exfiltration, groundwater evapotranspiration and net recharge. For instance, a study by Hassan et al. (2014) compared the advantage GSFLOW integrated hydrological model with standalone MODFLOW solution by (Lubczynski & Gurwin, 2005) in the same catchment and based on nearly the same conceptual model. The authors found that the two modeling budgets were quite different mainly because of the importance of groundwater exfiltration in GSFLOW solution. The standalone MODFLOW distribute the gross recharge as groundwater evapotranspiration or as groundwater outflow to the nearest sink boundary while in GSFLOW, the gross recharge can be dynamically exfiltrated to the shallow soils. Moreover, groundwater evapotranspiration is significantly higher loss in arid and semi-arid (Lubczynski, 2006) but not considered in studies of UTB with standalone groundwater modeling. Neglecting such quantifications of spatio-temporal water fluxes which are more dependent on hydrological driving forces particularly in arid and semi-arid areas may affect water resource management.

Therefore, this study, under Ethiopian Education Network to Support Agricultural Transformation (EENSAT) project, will integrate spatio-temporal information and earth observation techniques to investigate water resource responses to LULC dynamics.

1.2. Research problem and justification

Due to erratic and a non-linear rainfall distribution, water shortage is a big challenge in Ethiopia. As a result, GTP of the country clearly stipulates intensification of agricultural practices particularly within River Basins, including the Tekeze Basin to ensure food security. According to the national GTP-II, irrigation is planned to increase by about 56% from 2015/2016 to 2019/20. This will be continued to realize the national vision of becoming a low middle income country by 2025. Such plan requires dynamic LULC change because of the dynamic population growth and competition to available land and this can affect the water resources spatially and temporally. Particularly, the northern Ethiopia has experienced complex changes in LULC pattern and can be continued to the future (Teka et al., 2013).

The water shortage remains a prevalent problem in the semi-arid Upper Tekeze Basin (UTB) due to the short duration of the rainy season and high rainfall variability. This has been resulted in recurrent droughts (eg. Philip et al., 2018) and the groundwater is also affected, especially in the dry season, with many wells getting drier. Springs which are representative of the productivity of aquifers in UTB also significantly decrease their discharge in mid months of dry season and become totally dry in the late months of the dry season (Girmay et al., 2015). On top of this, the GTP envisages more intensive agricultural practices and LULC changes taking UTB as developmental corridor. The future LULC can exacerbate the water shortage by affecting the complex water fluxes in the surface and groundwater domains. Conversely, LULC change impact on spatio-temporal surface-groundwater interaction is not well investigated. The relationship among the main hydrological driving forces (rainfall and potential evapotranspiration) and the water fluxes under geologically varied and topographical complex of UTB are also not well known. This requires in depth investigations of the spatio-temporal surface-groundwater interactions and groundwater resources changes. This can be realized through the application of an integrated hydrological models. However, the poor coverage of ground-based hydro-meteorological gauging stations challenged application of the integrated hydrological models. Particularly, lack of the rainfall and potential evapotranspiration at required spatio-spatial resolution hinders these applications.

The UTB is characterized by high temporal and spatial variability of rainfall (Gebremicael et al., 2017). The geographical location of rainfall stations in this study area are not spatially well distributed because they are placed based on access suitability i.e. on the village towns of the Basin. Hence, they are not representative to the spatial requirement of integrated hydrological mode. Remote sensing derived products are becoming as an alternative sources of data. However, their application in integrated hydrological is rare because of their systematic error and resolution (Camici et al., 2018). Potential evapotranspiration is also another driving input to water resource studies. The common standard approach to compute potential evapotranspiration is to use climatic data from ground meteorological stations. However, representative weather stations to measure climatic variables for the calculation of potential evapotranspiration in UTB are limited. Similar to the rainfall, advancement of remote sensing can be used as an alternative source but the performance of satellite derived potential evapotranspiration has not been validated in UTB for integrated hydrological model.

Therefore, this study proposes to apply satellite derived rainfall and potential evapotranspiration products to address the data scarcity and quantify spatio-temporal water resource responses to LULC change in the semi-arid UTB of Northern Ethiopia. This study will contribute to sustainable water resource management and as a pilot study that can be followed in other Basins in Ethiopia.

1.3. Scope of the study

The study area covers semi-arid UTB which is also area of interest by the EENSAT project. Assessing the spatio-temporal water resources in UTB is crucial for sustainable water resource management. Therefore, this study will cover three main interrelated components. Firstly, validating and merging satellite derived rainfall and potential evapotranspiration estimations. Secondly, conceptualize and calibrate integrated hydrological model to quantify the surface-groundwater interactions and groundwater resources in a spatio-temporal manner. Thirdly, predict water resources changes under future LULC changes.

1.4. Research objectives and research questions

Research objectives

The aim of this study is to conceptualize and quantify spatio-temporal water resources and their response to LULC in the semi-arid UTB in Northern Ethiopia. The following specific objectives are formulated to achieve the main objective.

I. Validate and merge daily satellite derived rainfall and potential evapotranspiration estimations
II. Setup and calibrate an integrated hydrologic model to quantify spatio-temporally surface-groundwater interactions and groundwater resources
III. Predict future water resources changes in response to future LULC change

Research questions

The research questions for each of the specific objectives are as follows:

I. Validate and merge daily satellite derived rainfall and potential evapotranspiration estimations for the UTB
    - What is the temporal and spatial performance of satellite derived rainfall estimates in semi-

arid area with complex topography?

- What is the temporal and spatial performance of satellite derived potential evapotranspiration estimates in semi-arid area with complex topography?
- How can the satellite derived rainfall estimates be integrated with in-situ observations for improved bias correction?
- How can the satellite derived potential evapotranspiration estimates be corrected with in-situ observations?

II. Setup and calibrate an integrated hydrologic model to quantify the surface-groundwater interactions and groundwater resources in the UTB

- What is the hydrogeological conceptual model to represent the surface groundwater interaction?
- How surface-groundwater interaction is characterized spatially and temporally?
- What is the spatio-temporal variability of net recharge and aquifer storage in response to different LULC?

III. Predict future water resources changes in response to future LULC change in the UTB

- What is the past trend in LULC change?
- What are the main driving factors for LULC change and how could be prioritized?
- What is the predicted LULC change dynamics?
- How sensitive is the water resources change in response to future LULC change?

1.5. Research assumptions

- Integrating satellite derived rainfall and potential evapotranspiration with in-situ observations in relation to topography improves the accuracy of the satellite products
- Groundwater flow pattern matches the surface watershed divide of the UTB
- Integrated hydrological model can successfully simulate the spatio-temporal characteristics of water fluxes and detail water balance of UTB
- LULC change affects the surface-groundwater interaction and aquifer storage of UTB

1.6. Research originality

This study is expected to add knowledge of using various satellite based products as input of integrated hydrological models to quantify spatio-temporal water resources.

- Satellite derived rainfall and potential evapotranspiration have not been validated and integrated to in-situ observations and applied within an integrated hydrological model in UTB
- The impact of future LULC changes on surface-groundwater interactions using integrated hydrological modeling has not been addressed in UTB

1.7. Conceptual framework

This study will apply a research approach consisting of the components and their relationships presented in in Figure 1-1. Satellite based hydrological driving forces will be validated and improved at the UTB. Conceptual model development, setup and calibration of integrated hydrological model to quantify the spatio-temporal surface-groundwater interactions and groundwater resources will be followed. Past and current LULC will be analyzed and then the future LULC will be predicted based the past LULC trend and given scenarios. Finally, the future water resources in response to future LULC changes will be predicted and analyzed.

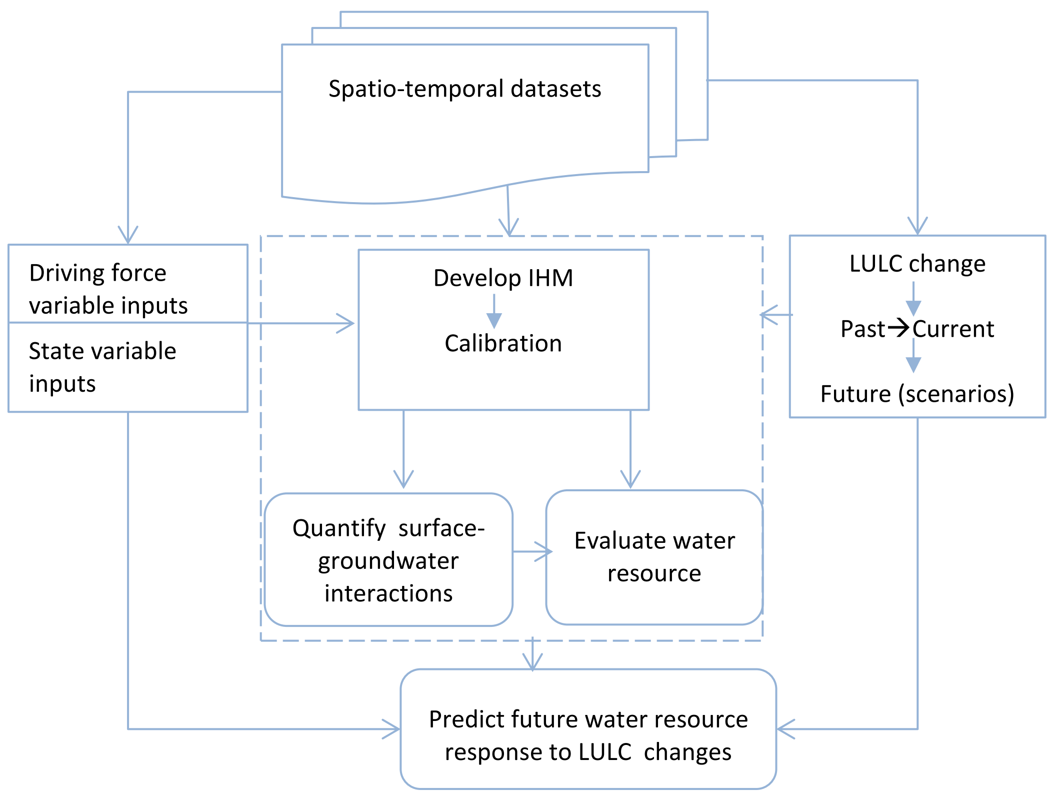

Figure 1-1 Research conceptual framework

2. Study area

2.1. Location and topography

Tekeze River Basin is one of the 12 main river basins in Ethiopia which covers parts of the Amhara and Tigray regional states. Tekeze Basin has a potential for large scale irrigation sites with an estimated potential irrigable area of 83,368 hectares (Awulachew et al., 2007). Zamra Catchment of UTB is selected for this study. The study area is located in northern Ethiopia between latitudes of 12° 38′ 12″ and 13° 20′ 16″ N and longitudes of 38° 59′ 23″ and 39° 40′ 05″ E (Figure 2-1). The study area covers about 3500 km^2. Based on topographic information, from the Shuttle Radar Topographic Mission (SRTM) Digital Elevation Model (DEM), the elevation of the study area ranges from 1230 m to 3948 m above sea level with mean elevation of 2148 m. The highest elevation lies in the southeast parts of the study area with lowest elevation at the western discharge outlet. More than 50 % of the study area is having slopes of less than 15^0 and about 12 % of the study area is very steep sloping (greater than 30^0).

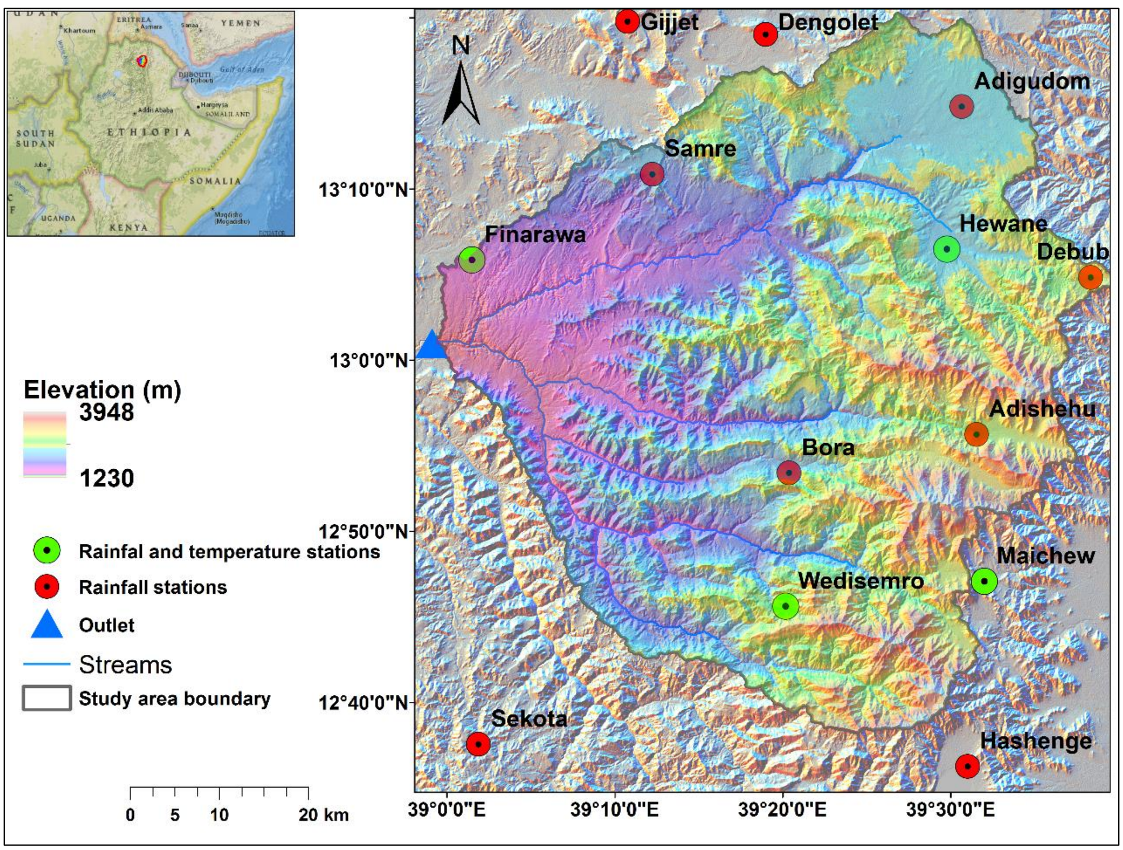

Figure 2-1: Location map of study area

2.2. Climate

The rainfall of the study area is variable spatially and temporally with the high rainfall in the eastern mountain areas. According to the data for 2000-2009 from 8 stations, the mean annual rainfall varies from 424 mm to 880 mm. The climate is a semi-arid with rainfall restricted to the main short rainy season period from June to September with a maximum of 290 mm during August (Figure 2-2). The mean monthly temperature for the same period with rainfall also varies in line with the elevation of the study area. The mean monthly temperature varies from about 13 ^{0}C in the eastern mountain station to about 28 ^{0}C in the western low elevation of the study area (Figure 2-3).

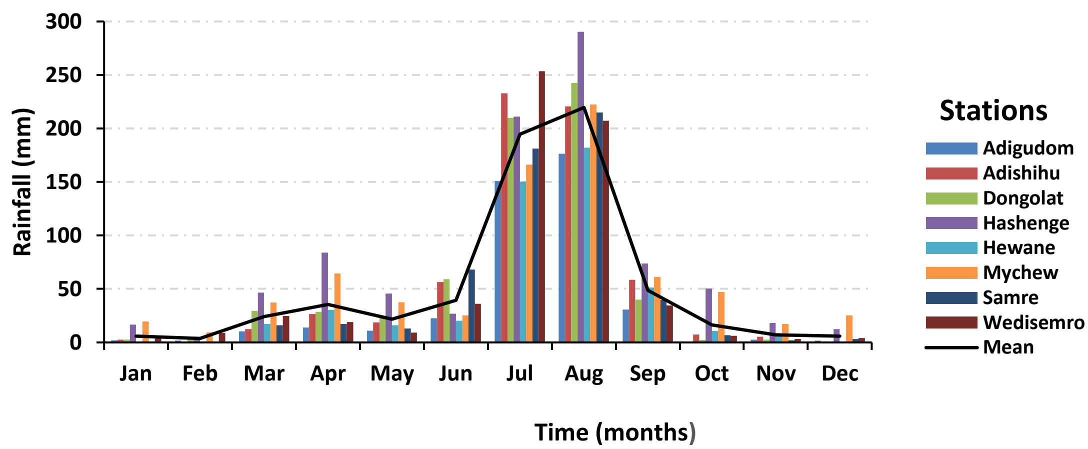

Figure 2-2: Mean monthly rainfall of the study area (2000-2009) for eight stations as listed in Figure 2-1

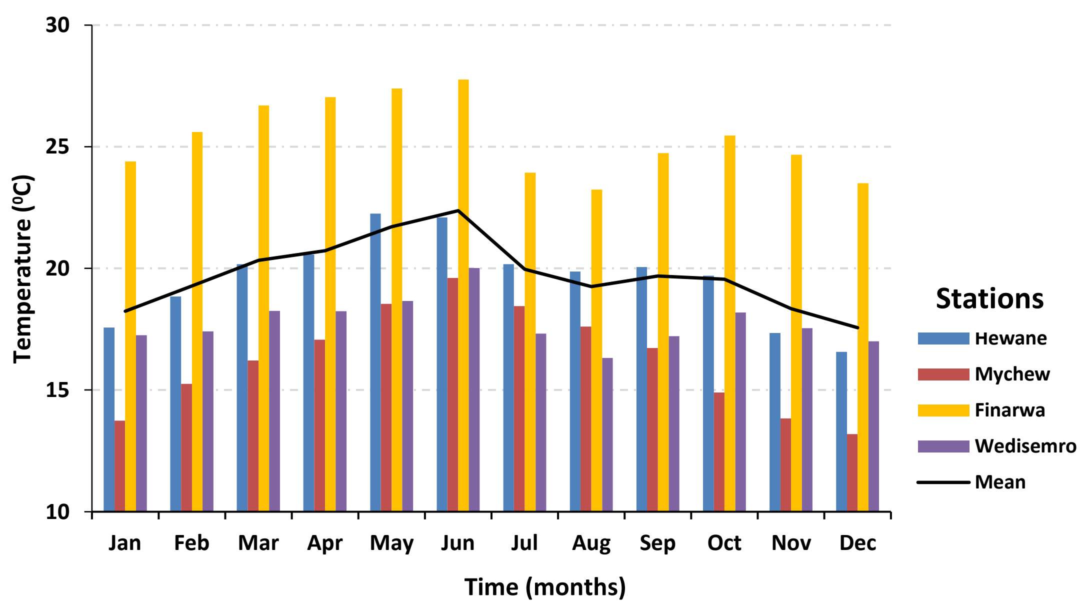

Figure 2-3: Mean monthly temperature of study area (2000-2008) from four stations as listed in Figure 2-1

2.3. Geology

The geological formations of study area is characterized by precambrian basement, Enticho Sandstones, Adigrat Sandstone, Antalo Limestones, Agula Shales, Ambaradom Sandstone, Mekele Dolerites, Ashangie Formation, Alaje Formation (Sembroni et al., 2017; Geological Map of Ethiopia, 2011). The Ashengie and Alajie formations are under the basalt sequence hydrostratigraphic unit (Kebede, 2013). Ashengie formation a geological formation with rugged topography, thinly bedded, with cross cutting dykes, deeply weathered, low permeability, dissected and irregular morphology. Alajie formations are marked by low degree of weathering, thick layering, and cliff forming topography under the fractured and weathered zones. These formations are important recharge zones in which groundwater could be tapped through hand-dug wells and springs.

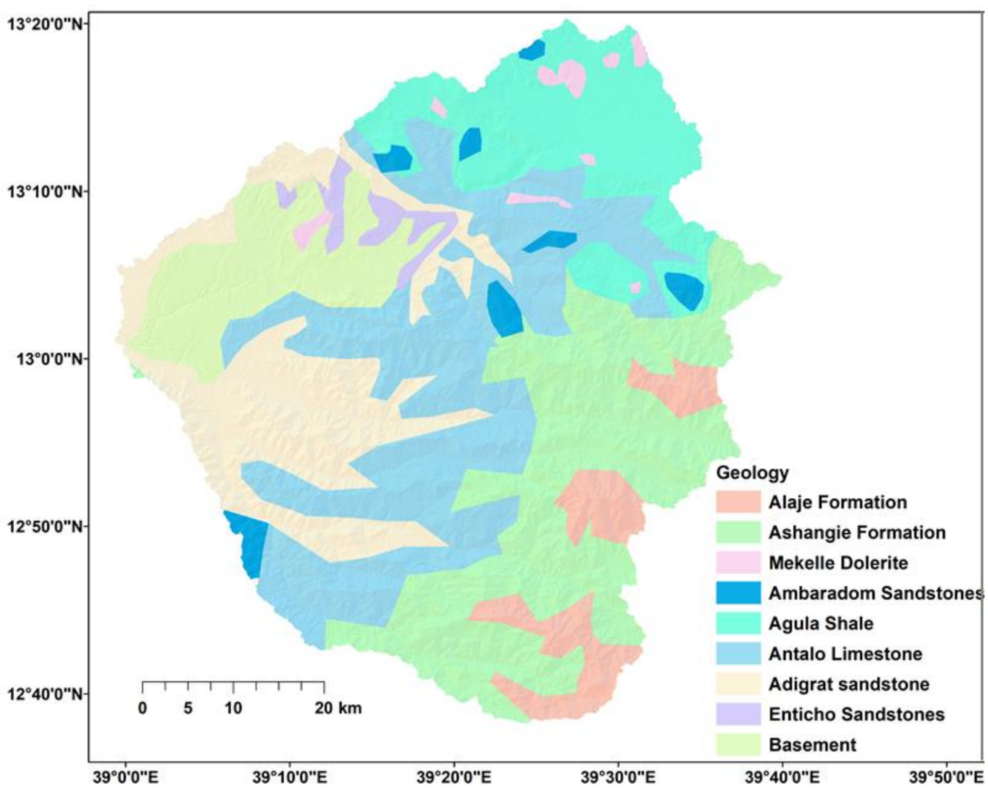

Figure 2-4: Geological map of study area (after Sembroni et al., 2017 and Geological map of Ethiopia, 2011)

2.4. Soil

The study area is dominantly with sandy loam soil texture followed by clay to the west and north part and very small part in the north east is loamy sand. In terms of soil type, Lithic Leptosols are dominantly covered the volcanic and limestone formations of the study area (Figure 2-5). The Agula Shell formation in the northern part of the study area is covered with Vertic Cambisols. The basement and parts of sandstone formations of the study area are covered with Chromic Cambisols.

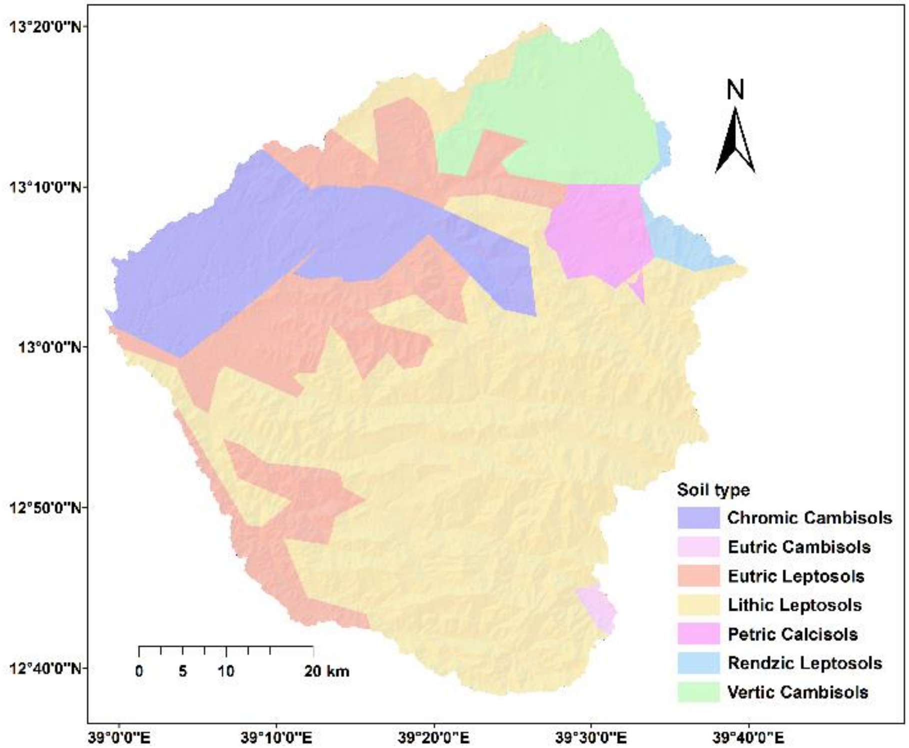

Figure 2-5: Soil type of study area (after EthioSIS)

2.5. Land use land cover

Land cover derived from the Africa Soil Information Service (AfSIS) Moderate Resolution Imaging Spectroradiometer (MODIS) Collection is compared for the years 2001 and 2012. AfSIS MODIS Collection Land Cover Type 2 data set is constructed for the continent of Africa using observations beginning in February 2000 from the National Aeronautics and Space Administration (NASA). The grids have an annual temporal resolution with a spatial resolution of 500 meters. According to the AfSIS MODIS Collection Land Cover type, the savannas showed a dramatic decrement change and the crop lands showed increment from 2001 to 2012. Grass lands also showed a decrement while the shrub land showed increment. A land cover map is also obtained from ESA Climate Change Initiative-Land Cover (CCI-LC) project at 20m over Africa based on 1 year of Sentinel-2A observations from December 2015 to December 2016 (prototype). According to CCI-LC land cover classification, the study area is dominantly covered with cultivated land followed by grassland and shrubland. The classification of the aforementioned sources is to provide an overview of the LULC change in the study area. The proportion change may not represent the actual change on the ground as they are constructed at regional level. These data sets are to show the preliminary LULC changes from existing sources and will not be used as input for modeling because LULC classification and prediction will be applied at study area level with ground truth verification. A study by Welde & Gebremariam (2017) also shows that the land use types in the study area are cultivated, bare land, forest and woodland, shrubland, grass land dominantly covered with shrub land and cultivated land.

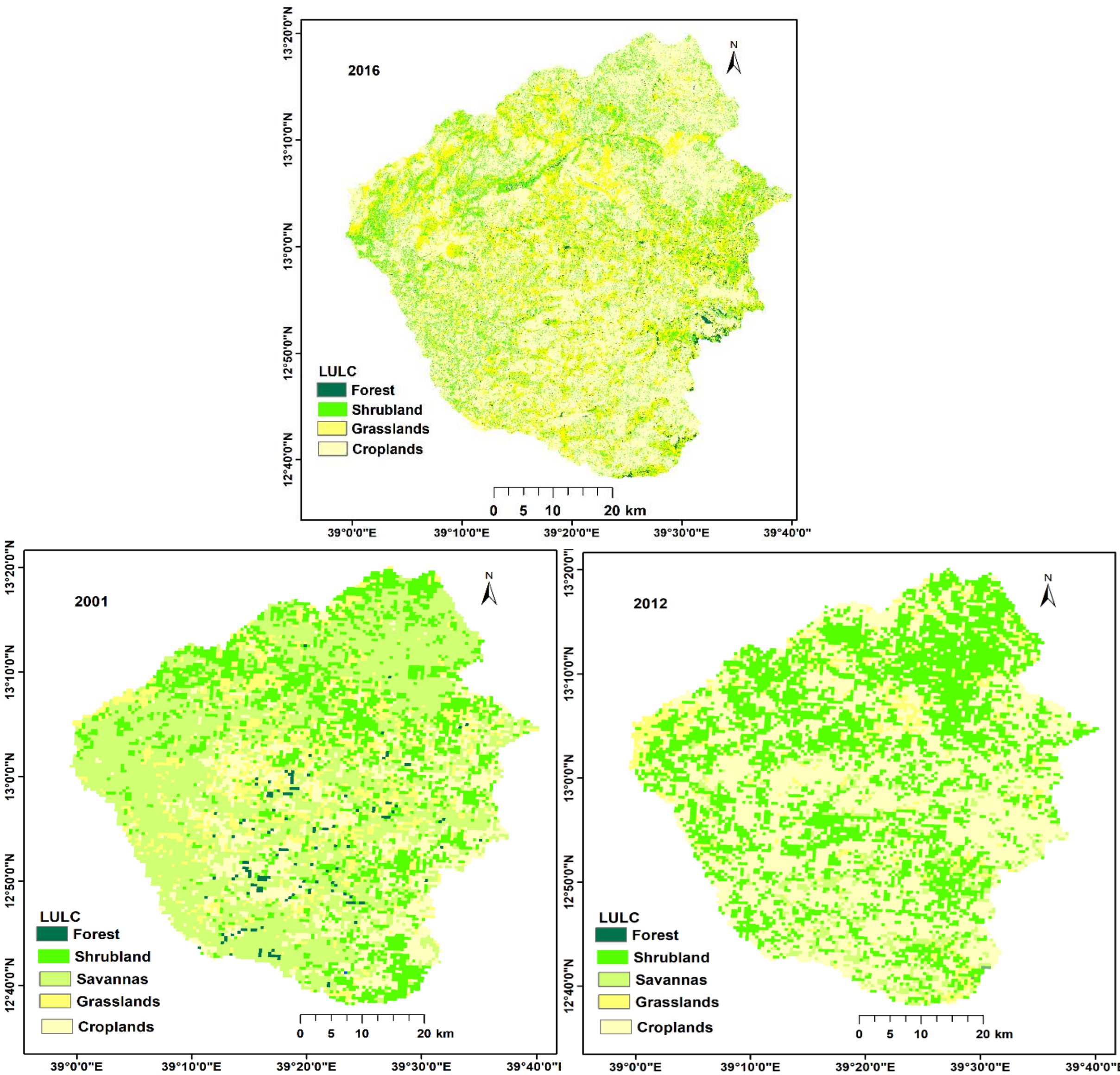

Figure 2-6: LULC of study area for 2001, 2012 (AfSIS MODIS) and 2016 (ESA CCI-LC).

2.6. Drainage networks and hydro-geology

This study area is adjacent to Tsirarie Catchment in the south west and Arequat Catchment in the north west. The topography is characterized by highlands in the Eastern and decrease to the West with rivers that flow towards the western part of the Catchment. Peak flow is in the summer time due to overland flows and continuous base flow in the dry season. The drainage pattern is a dendritic system that flows following the slope and topography and joins as tributaries to the main river at around 4 km before the outlet as shown in Figure 2-1.

The study area has many springs particularly in the summer season and relatively shallow groundwater. The shallow groundwater system is recharged from precipitation in the highland plateaus and it discharges through springs and baseflow to river. The aquifer in the study area is simplified as diverse productive aquifers in the volcanics, aquifers in the sedimentary rocks mainly existing along river valleys and shallow less productive aquifers in the basement rocks (Girmay, 2015).

3. Validating and improving satellite rainfall and potential evapotranspiration estimations -Objective-I

3.1. Introduction

Hydrological models are important tools to simulate and predict water resources on the Earth for establishing reliable water resources management system taking rainfall and potential evapotranspiration as main driving force inputs. Therefore, evaluating and improving of these driving forces at fine spatial and temporal scale is important to understand the hydrological characteristics for effective water resources management (Habib et al., 2014; Rahmawati and Lubczynski, 2017; Zambrano-Bigiarini et al., 2017; Lekula et al., 2018).

Though good quality and distribution rainfall data is a prerequisite for modelling applications, the meteorological stations in Sub-Saharan Africa networks are not well enough distributed (Luetkemeier et al., 2018) particularly in mountainous areas where the high rainfall and variability takes place (Rahmawati and Lubczynski, 2017). As a result, there is a limitation in estimating accurate rainfall at adequate spatial distribution (Kimani et al., 2017). Rainfall records from gauging stations are also not capable of detecting at the reasonable resolution required by hydrologic applications due to limitation to capture spatial and temporal variability and low quality of measurement instruments (Habib et al., 2009). Satellite rainfall products are particularly valuable for regions with a lack of distributed in-situ measurements because of their availability for free and unlimited by administration factors (Hu et al., 2015). Therefore, the satellite derived rainfall estimations can be an alternative way to overcome the gap of observed rainfall data scarcity especially in remote and inaccessible areas in Ethiopia where rain gauge stations are not representative (Dinku et al., 2014). Despite the improvement of satellite derived rainfall products for several applications, a site specific validation has to be performed before using for hydrological studies (Zambrano-Bigiarini et al., 2017) because their accuracy varies from region to region (Fenta et al., 2018).

Thermal Infrared (TIR) and Passive Microwave (PMW) sensors are the commonly used algorithms to retrieve rainfall from satellites (Kidd, 2001). The TIR based rainfall rates are inferred from cloud top temperatures assuming that rainfall and cold cloud duration are linearly correlated. The PMW based approach provide the rainfall rates by penetrating clouds to explore their internal properties through the interaction of raindrops with the radiation field which is perceived as their strong side. TIR and PMW have their own limitations. TIR radiation are limited to penetrate clouds, underestimates warm rain and weak performance to identify cirrus clouds from rain clouds (Kidd, 2001; Thiemig et al., 2013; Dinku et al., 2014). PMW have also the limitation to detect warm orographic rains and very cold surfaces like mountain tops covered by ice can be detected as rainfall (Toté et al., 2015). To overcome these limitations, the recent satellite derived rainfall products combine TIR and PMW to estimate rainfall at finer spatial and temporal resolutions (Ayehu et al., 2018; Worqlul et al., 2018) and nowadays also forecasts are used.

Some studies validated satellite derived rainfall by comparing the in-situ point station records with pixel rainfall values at different temporal scales (Table 3-1). However, most satellite rainfall studies rely to Blue Nile Basin and findings showed that both over and under estimations of rainfall with different accuracy levels. This variability may be because of their dependency on topography and local climate variability which is an indication for local validation of satellite derived rainfall estimations. Merging of satellite derived rainfall with locally available in-situ observations are recommended as an approaches to overcome such biases (Dinku et al., 2011). As a result, there is one initiative called Enhancing National Climate Services (ENACTS) that integrate satellite and in-situ rainfall at national and regional level but basically for characterization of climate risks (Dinku, et al., 2018). Therefore, validating and merging of satellite derived rainfall product can better represent the poor distribution of station networks in UTB .

Table 3-1: Summary studies on satellite rainfall validation over parts of Ethiopia

Product	Reference	Remarks
RFE, TRMM-3B42*, CMORPH*, PERSIANN	Dinku et al. (2008)	Poor in estimating the amount of rainfall in each pixel
CMORPH*, TRMM-3B42*, ARC	Dinku et al. (2011)	Moderate underestimation in highlands and high over estimation over dry region dry
CMORPH*, TRMM-B42RT, 3B42* and PERSIANN	Bitew et al. (2012)	Significant biases in the satellite rainfall estimates
CMORPH	Haile et al. (2013)	Could not capture the rainfall temporal variability
CMORPH	Habib et al. (2014)	Bias correction improve accuracy of the product
TRMM-3B42*, MPEG*, CFSR	Worqlul et al. (2014)	overestimation and underestimation varies spatially
CHIRPS*, ARC2, TAMSAT*	Dinku et al. (2018)	Exhibits spatial and temporal performance variability
CHIRPSP*, TAMSAT* and ARC 2	Ayehu et al. (2018),	Exhibits spatial and temporal performance variability
CHIRPS*, TAMSAT* and ARC 2	Fenta et al. (2018)	Exhibits spatial and temporal performance variability

*relatively better performance

Potential evapotranspiration is another driving force to hydrological models representing the upper limit of the evaporation rate (Oudin et al., 2010) and understanding its effect on water resource is crucial for efficient water resources planning and management (Cleugh et al., 2007). Potential evapotranspiration has been estimated using different developed methods in the past decades (Bai et al., 2016). These includes such as Hargreaves Samani (Hargreaves & Samani, 1985), Priestley Taylor (Priestley & Taylor, 1972), Makkink (De Bruin & Lablans, 1998), Penman-Monteith (Allen et al., 1998). Different potential evapotranspiration estimation methods can behave differently and the estimated values are not always in agreement with each other because of the different assumptions and input requirements of each method (Allen et al., 1998). Methods of evapotranspiration estimation can be grouped in to three based on their input requirement (Bai et al., 2016). These are temperature based methods, radiation based methods and radiation and aerodynamic based methods. The temperature based required temperature only as input to compute potential evapotranspiration (Shaw & Riha, 2011; Sheffield et al., 2012). Radiation based methods are based on the energy balance and require solar radiation and temperature as inputs (Xu & Singh, 2000). The radiation and aerodynamic based methods compute potential evapotranspiration based on more reliable physical processes but require more meteorological variables as input (Allen et al., 1998). Many studies have compared these methods including their sensitiveness to hydrological model (Bai et al., 2016). However, there are some conflicting results on sensitiveness different potential evapotranspiration methods to hydrological models. In general the radiation and aerodynamic based methods are the more robust method to accurately estimate potential evapotranspiration. Despite their limitation and strong side of these methods, it is still a challenge to obtain the input from ground measurement at representative spatial scale to compute potential evapotranspiration. Moreover, spatially representative estimation of ground based potential evapotranspiration is not reliable because it is costly to install instruments that measure accurate evapotranspiration across river basins (Karimi and Bastiaanssen, 2015). Therefore, shifting to satellite based potential evapotranspiration as alternative can be used to overcome the data scarcity and inconsistency of ground based measurement (Kim & Hogue, 2008).

Therefore, this study will validate and improve satellite derived rainfall and potential evapotranspiration estimations at relatively high spatial and temporal scale which will be used as driving force inputs for integrated hydrological modelling application. Moreover, it can provide information to potential users interested on these products like in suitable estimates of irrigation requirements to support of water management in the study area.

3.2. Data acquisition

Ground-based data and remote sensing data will be sourced to address the research questions under validating and merging of satellite rainfall and potential evapotranspiration.

3.2.1. Ground-based data

Daily meteorological data within the study area and from nearby stations will be obtained for the time period of 2015-2018 from the Ethiopian National Meteorological Agency (NMA) but most of these stations are non-recording. Data quality will be checked for consistency and homogeneity. Furthermore, there are inconsistencies on the geographical coordinates of stations from NMA and different published literatures. Therefore, geographical locations of the meteorological stations will be verified during field work. Additional automatic weather stations will be installed that record all climatic variables including rainfall, air temperature, relative humidity, sunshine hour, wind speed and direction to compute potential evapotranspiration. Double-mass curve technique (Searcy and Hardison, 1960) will be applied to test the consistency of the meteorological data.

3.2.2. Remote sensing data

Rainfall

The satellite rainfall from the grids that cover the study area will be downloaded via the GEONETCast reception station at International Institute for Geo-Information Science and Earth Observation (ITC) /Mekelle University for the same time period with the ground based data. Spatio-temporal scale and complexity of topography can be a cause to relatively poor agreement between satellite derived rainfall estimation and in-situ measurements. Satellite rainfall products with relatively high spatio-temporal scale can minimise the difference error with in-situ observations (Rahmawati & Lubczynski, 2017). Moreover, Dinku et al. (2014) remarked that local merging of satellite estimates with all locally available in-situ rainfall method could improve the accuracy of satellite products. Therefore, this study will use satellite products with relatively high spatio-temporal resolution. These are the Multi-Sensor Precipitation Estimate-Geostationary (MPEG) satellite and Climate Hazards Group Infrared Rainfall with Stations (CHIRPS).

MPEG rainfall is produced by the European Organisation for the Exploitation of Meteorological Satellites (EUMETSAT) meteorological product extraction facility (MPEF). MPEG is derived from the infrared data of the EUMETSAT geo-stationary satellites by continuous re-calibration of the algorithm with rain rate data derived from polar orbiting microwave sensors (Worqlul et al., 2018). The algorithm is based on a combination of Meteosat Second Generation (MSG) images from the infrared IR10.8 μm channel and passive microwave data from the Special Sensor Microwave/Imager (SSM/I) instrument on the United States Defence Meteorological Satellite Program (DMSP) polar satellites. The MPEG data are available through the GEONETCast near-real-time global network of satellite-based data dissemination systems designed to distribute space based, air-borne and in-situ data. This product with relatively high spatial resolution (3km) and high temporal resolution (15 minute) will be sourced freely from the ITC ftp server: ftp://ftp.itc.nl/pub/.

CHIRPS is a new quasi-global (50^o S–50^o N) gridded product with spatial resolution of 0.05^o and temporally at daily, pentadal, dekadal, and monthly resolution (Funk et al., 2015). CHIRPS algorithm takes the advantage of integrating data sources from the Climate Hazards group Rainfall climatology (CHPclim), TIR-based satellite rainfall and in-situ measurement. The CHPclim is a global rainfall climatology that uses long-term average satellite rainfall fields as a guide to deriving climatological surfaces which could improve its performance with complex topography like Ethiopia (Funk et al., 2015). Similar to MPEG, CHIRPS rainfall product at about 5km resolution will be freely accessed from Climate Hazards Group link http://chg.ucsb.edu/data/index.html or via ITC ILWIS In Situ and Online Data Toolbox (ISOD): ftp://chg-ftpout.geog.ucsb.edu/pub/org/chg/products/CHIRPS-2.0/global_daily/tifs/p05/.

Evapotranspiration

For the satellite based evapotranspiration, Land Surface Analysis (LSA) Land Surface Temperature (SAF) daily Reference Evapotranspiration (DMETREF) and Daily MSG Evapotranspiration (DMET) evapotranspiration will be used. The LSA SAF DMETREF provides daily reference evapotranspiration estimated from daily global radiation derived from Spinning Enhanced Visible and Infrared Imager/Meteosat Second Generation (de Bruin et al., 2016). While the DMET product obtained by temporal integration of instantaneous values represents the actual evapotranspiration. DMETREF and DMET products can be obtained from the LSA-SAF site link https://landsaf.ipma.pt/en/. For this study, these products will be sourced from the ITC server. This study will validate the METREF evapotranspiration using in-situ observations while the DMET evapotranspiration will not be validated because of unavailable actual evapotranspiration. DMET will be used to compare with model simulated actual evapotranspiration.

3.3. Methodology

Preparation and analysis of the daily satellite rainfall and potential evapotranspiration will be performed using the ILWIS open source Water and Food Security Ethiopia Toolbox (Maathuis et al., 2018). Performance of satellite derived rainfall have to be validated with ground observations before proceeding to their application (Rahmawati & Lubczynski, 2017; Kimani et al., 2017; Lekula et al., 2018). As such, this study will validate these satellite products at different temporal scales and merging of the satellite rainfall and in-situ observed rainfall will be applied to improve the accuracy of satellite derived rainfall.

3.3.1. Rainfall evaluation

Performances of satellite rainfall will be evaluated before and after bias correction at different temporal scales against in-situ observations using graphical techniques and statistical methods. Descriptive statistics, categorical statistics and bias decomposition methods will be applied to evaluate the performance of satellite rainfall product (Ayehu et al., 2018; Dinku et al., 2018; Lekula et al., 2018).

The descriptive statistics will be used to compare the satellite derived rainfall with in-situ rainfall observations. The descriptive statistics to be used in this study include: i) Pearson's product-moment correlation coefficient (r) ii) Mean Error (ME); iii) Mean Absolute Error (MAE) and iv) Mean Square Error (RMSE). The equations of the aforementioned descriptive statistics are as follows.

$$r = \frac{\sum_{i=1}^{T}\left(Gr_i - \bar{Gr}\right)\left(Sr_i - \bar{Sr}\right)}{\sqrt{\sum_{i=1}^{T}\left(Gr_i - \bar{Gr}\right)^2}\sqrt{\sum_{i=1}^{T}\left(Sr_i - \bar{Sr}\right)^2}} \quad (3.1)$$

$$ME = \frac{1}{T}\sum_{i=1}^{T}\left(Sr_i - Gr_i\right) \quad (3.2)$$

$$MAE = \frac{1}{T}\sum_{i=1}^{T}\left|Sr_i - Gr_i\right| \quad (3.3)$$

$$RMSE = \sqrt{\frac{1}{T}\sum_{i=1}^{T}\left(Sr_i - Gr_i\right)^2} \quad (3.4)$$

Where Gr_i is in-situ rainfall; Sr_i is satellite rainfall; the over bar Gr_i and Sr_i represents for the average in-situ and satellite rainfall respectively; T is the total number of given temporal data pairs. The range of values in *r* is from +1 to -1 in which a value of 0 indicates that there is no association between the two rainfall values and a value 1 indicates perfect correlation; The *ME* value ranges from -∞ to ∞ with perfect score at 0; *MAE* and *RMSE* values range from 0 to ∞ with perfect score at 0. Negative values indicate underestimation while positive indicate overestimation.

The categorical statistics are also another common way to evaluate detection capabilities of satellite rainfall (Lekula et al., 2018). Accordingly, the categorical statistics to be applied in this study includes: i) Probability of Detection (*POD*); ii) False Alarm Ratio (*FAR*); iii) Critical Success Index (*CSI*); iv) Frequency

Bias (*FBS*) V) and Heidke skill score (*HSS*). These statistics are computed based on the combinations between satellite derived rainfall and in-situ observations to verify the frequency of the correct and incorrect rainfall detection at a given temporal resolution. The four combinations are Hit (satellite and in-situ measured rainfall vales), Miss (no estimation rainfall from satellite but in-situ measured rainfall), False alarm (satellite estimated rainfall but no measured value in in-situ rainfall) and Correct negative (no rainfall estimation from satellite and in-situ stations).

Table 3-2: Contingency matrix for frequency of rainfall detection

	In-situ measured rainfall	No in-situ rainfall measured
Satellite rainfall detected	Hit (M)	False alarm (FA)
No satellite rainfall detected	Miss (M)	Correct negative (CN)

$$POD = \frac{H}{(H+M)} \quad (3.5)$$

$$FAR = \frac{FA}{(H+FA)} \quad (3.6)$$

$$CSI = \frac{H}{(H+FA+M)} \quad (3.7)$$

$$FBS = \frac{H+FA}{(H+M)} \quad (3.8)$$

$$HSS = \frac{2(H.CN - FA.M)}{(H+M)(M+CN)+(H+FA)(FA+CN)} \quad (3.9)$$

POD, ranges from 0 to perfect 1, is fraction that quantifies the proportion of observed rainfall days that are correctly estimated by the satellite product at given threshold. *FAR*, range from perfect at 0 to 1, is the proportion of satellite estimated rainfall days with no in-situ rainfall. *CSI*, ranges from 0 to perfect 1, is a proportion that satellite estimated rainfall correctly considering false alarms in contrast to POD. *FBS*, ranges from 0 to ∞, compares the satellite rainfall day detection frequency with the frequency of in-situ measurements: an *FBS* of less than (greater than) 1 indicates an underestimation (overestimation) of rainfall days. *HSS*, ranges from –∞ to 1, measures the overall skill of the rainfall estimates after rain events detected by random chance have been removed: *HSS* < 0 indicates that random chance is better than the satellite rainfall estimation; *HSS* = 0 means the satellite rainfall has no skill at all; and *HSS*= 1 indicates a perfect estimation of rainfall days by the satellite rainfall estimation. *HSS* takes the advantage over the other metrics because it measures the ability of the satellite to observe rain events relative to events that occur at random (Fenta et al., 2018).

The overall bias between satellite rainfall estimates and in-situ observed rainfall can be further decomposed to have more insight on the source of satellite rainfall errors (Habib et al., 2009). The total satellite derived rainfall bias will be decomposed in to Hit bias, Miss bias, False bias and Total bias. The first three bias analyses gives an insight in the possible source of satellite rainfall estimation algorithm error while the last bias indicates the cumulative difference between the satellite derived rainfall and in-situ measurements.

$$Hit\,bias = \sum_{i=1}^{T} \left(Sr_i - Gr_i\right) : \left(Sr_i > 0 \,\&\, Gr_i > 0\right) \qquad (3.10)$$

$$Miss\,bias = \sum_{i=1}^{T} Gr_i : \left(Sr_i = 0 \,\&\, Gr_i > 0\right) \qquad (3.11)$$

$$False\ bias = \sum_{i=1}^{T} Sr_i : \left(Sr_i > 0 \,\&\, Gr_i = 0\right) \qquad (3.12)$$

$$Total\,bias = Hit\,bias - Miss\,bias + False\,bias \qquad (3.13)$$

3.3.2. Merging satellite and in-situ rainfall

Despite of the high spatial applicability of satellite rainfall products, bias persists due to systematic errors. Therefore, it is crucial to correct the bias before applying to further applications. There are approaches, from simple bias adjustment to regression based relationships, to integrate satellite rainfall products and in-situ rainfall (Charlton & Fotheringham, 2009; Dinku et al., 2014; Hu et al., 2015; Chao et al., 2018). The most widely applied bias correction is mean bias correction i.e. multiplying the satellite rainfall by a factor from the ratio of in-situ rainfall to satellite rainfall (Lekula et al., 2018). However, mean bias correction assumes uniform bias over the spatial domain (Nerini et al., 2015). Moreover, such method may not reflect the non-stationary spatial relationship between satellite rainfall and in-situ rainfall due to the influence of land surface conditions and rainfall types (Lv & Zhou, 2016). As a result, merging the satellite rainfall with in-situ observed rainfall has been introduced to obtain rainfall with better accuracy at finer spatio-temporal coverage. It is a robust approach in improving the spatial resolution and quality of the satellite rainfall estimation particularly to use as input for hydrological modeling and other related applications (Wu et al., 2015; Ma et al., 2018; Chao et al., 2018).

This study will adopt geographically weighted regression (GWR) merging approach. GWR is an approach for exploring spatial heterogeneity in data relationships (Lu et al., 2014). GWR is a robust algorithm that has been used in satellite and in-situ rainfall merging approach (Charlton & Fotheringham, 2009; Hu et al., 2015; Chao et al., 2018). Moreover, GWR is more suitable to analyse the spatial relationship between rainfall and its influencing factors such as topography (Lv & Zhou, 2016).

Hu et al. (2015) expressed the general formula of GWR by Brunsdon et al. (1996) as follows:

$$Y_i = \beta_{i0} + \sum_{j=1}^{m} \beta_{ij}(u_i, v_i) X_{ij} + \varepsilon_i \qquad i = 1,2,\ldots,n \tag{3.14}$$

where Y_i and X_{ij} are dependent and j^{th} independent variable respectively at location i; u_i and v_i are the geographical coordinates; $\beta_{ij}(u_i,v_i)$ is the intercept, $\beta_{i0}(u_i,v_i)$ is the constant regression coefficient for X_{ij} and ε_i is the residual, m is the number of independent variables and n is the number of observations.

The satellite and in-situ rainfall merging approach will be performed with topography as influencing factor. The daily satellite rainfall will be first interpolated to 1km resolution, because the spatial resolution difference between point in-situ rainfall data and pixel satellite rainfall estimates can be the reason for overestimation or underestimation of rainfall by satellite products (Dinku et al., 2014). Topography as explanatory variables to GWR will be interpolated to the downscaled satellite rainfall spatial resolution. Then the difference between the in-situ rainfall and satellite rainfall at all stations will be computed as biases. Next, the GWR model will be used to estimate the spatial distribution of the biases with elevation as explanatory variables that affect the spatial distribution of rainfall (equation 3.15). Finally, the bias corrected rainfall will be produced by removing the spatial biases from the downscaled satellite rainfall at daily time step. The leave-one-out cross validation will be used to evaluate the accuracy of GWR algorithm and this will be iterated to the number of stations. The cross validation will be perforemed to evaluate the performance of GWR merging method, but all in-situ rainfalls will be used in the merging algorithm due to less number of stations. The descriptive statistics in (equation 3.1-3.4) will be then used to compare the merged and uncorrected satellite derived rainfall with in-situ rainfall observations.

$$B_i = \beta_{i0} + a_i T_i + \varepsilon_i \ldots\ldots\ldots\ldots\ldots\ldots\ldots\ldots\ldots\ldots\ldots\ldots\ldots\ldots\ldots\ldots . (3.15)$$

Where B_i is the bias between in-situ and downscaled satellite rainfall, β_{i0} is the constant regression coefficient, a_i is corresponding regression coefficient at location i, T_i is topography as explanatory variable, ε_i is the residual

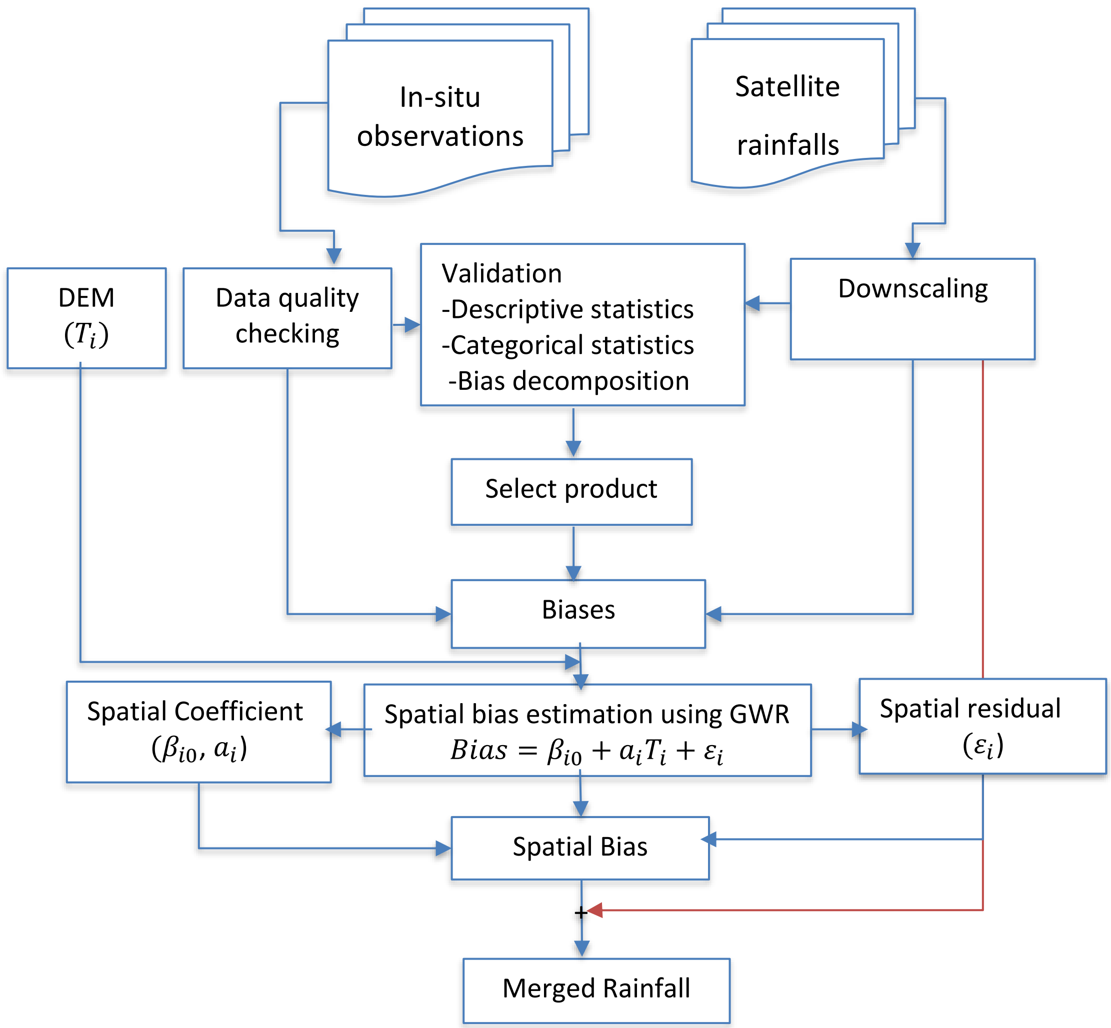

Figure 3-1: Flow chart of satellite rainfall evaluation and merging

Preliminary results

A short period two days from the rainy season is taken as sample to compare the in-situ observed rainfall with uncorrected CHIRPS and GWR merged rainfall. The correlation between uncorrected CHIRPS and GWR merged rainfall relative to in-situ observation at 8 rain gauge stations for August 26, 2015 shows with R^2 value less than 0.2 while for the GWR merged R^2 value is greater than 0.7 (Figure 3-2). This preliminary check is with linear regression only but other statistical evaluations need to be checked also for detailed comparison and evaluation of the merging approach at all time steps of the study period. The CHIRPS overestimated the observed rainfall and this improved after the GWR based merging approach. Moreover the CHIRPS rainfall shows a false alarm rainfall records in the northern and western stations of the study area on August 26, 2015 and this bias is improved after the CHIRPS is merged with in-situ observation using GWR merging approach. Another comparison between uncorrected CHIRPS and GWR merged rainfall relative to in-situ observation at 8 rain gauge stations for July 27, 2016 shows with R^2 value less than 0.4 while for the GWR merged R^2 almost near to perfect correlation (Figure 3- 3). This high correlation improvement might be due to the better correlation between the CHIRPS and in-situ observation compared to the correlation on August 26, 2015. Moreover, the GWR merging is applied for hit combinations of the CHIRPS and in-situ observation in all rain gauge stations.

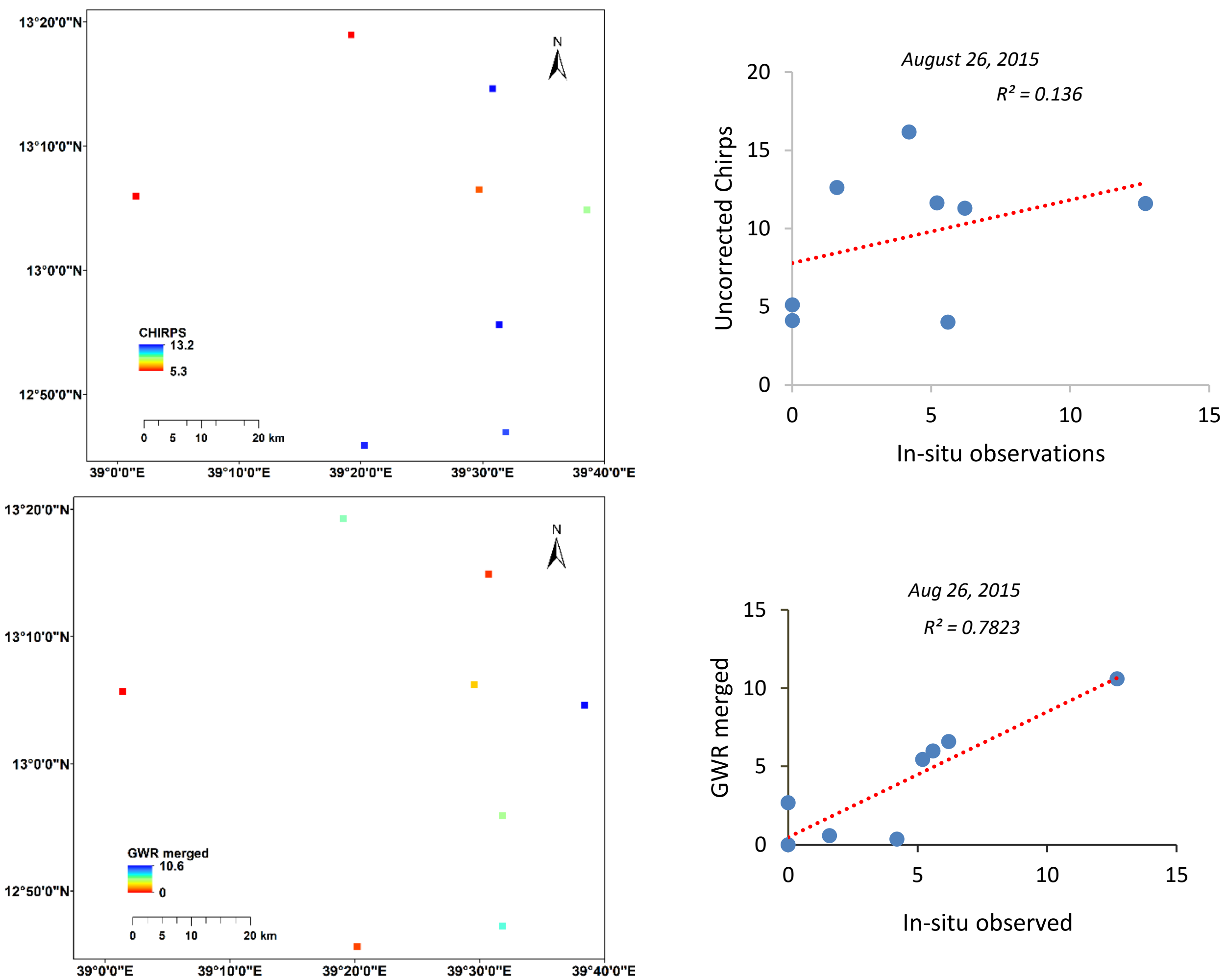

Figure 3-2: Uncorrected CHIRPS and GWR merged rainfall relative to in-situ observation at 8 rain gauge stations for August 26, 2015.

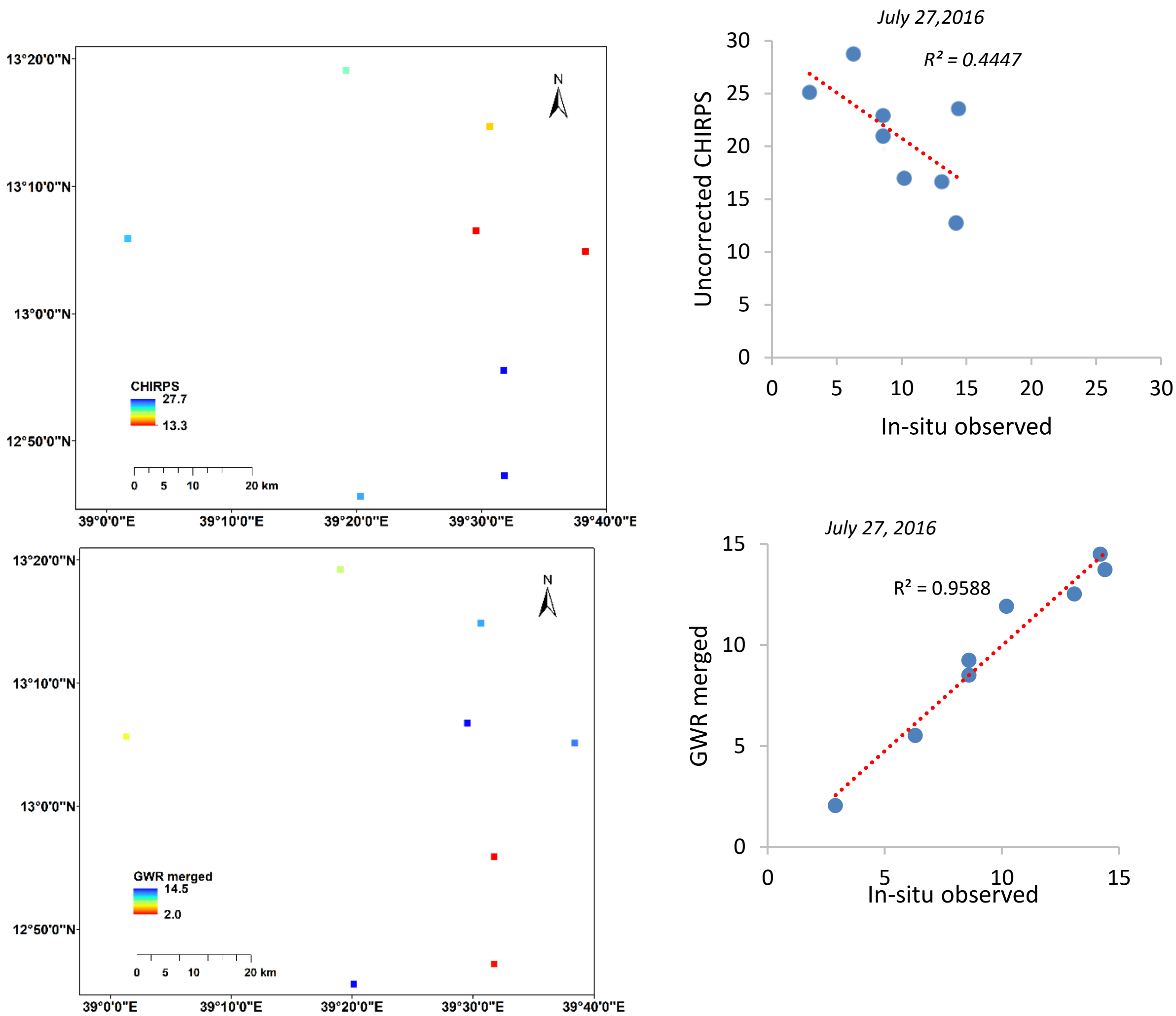

Figure 3- 3: Uncorrected CHIRPS and GWR merged rainfall relative to in-situ observation at 8 rain gauge stations for July 27, 2016

3.3.3. Potential evapotranspiration evaluation and correction

Nowadays satellites are providing evapotranspiration at high observation frequency (Ghilain et al., 2011). The high temporal resolution (eg. one observation every 30 min or even 15 min, in the case of METEOSAT Second Generation (MSG) satellites) is particularly interesting to monitor quickly evolving variables as a function of diurnal cycle and cloudiness. Now a MSG satellite is positioned at 41.5 degree, and Ethiopia is situated nearly sub-satellite. Therefore, the LSA-SAF DMETREF with high observational frequency will be validated for this study. The validation will be against potential evapotranspiration derived from Penman-Monteith method by Allen et al. (1998) at UTB to overcome the challenge on potential evapotranspiration estimation. This DMETREF product is a reference evapotranspiration from a clearly defined reference surface with the concept introduced to allow the estimation of the evaporative demand of the atmosphere independently of crop type, crop development or management practices (LSA LISA Team, 2016). The algorithm (equation 3.16) for LSA SAF DMETREF (Bruin et al., 2016) stated is valid for the reference grass surface assumption defined in FAO56 report (Allen et al., 1998). This method combines daily global radiation data derived from geostationary satellite data and daily average air temperature at 2 m obtained from European Centre for Medium-Range Weather Forecasts (ECMWF) forecasts to estimate the DMETREF (Figure 3-4).

$$\mathrm{DMETREF} = \frac{1}{\lambda}\left[\frac{\Delta}{\Delta+\gamma}Q^{*}+\beta\right] \dots\dots\dots\dots\dots\dots\dots\dots\dots\dots\dots\dots\dots\dots. (\mathbf{3.16})$$

where λ is the latent heat of vaporization, Δ is the slope of saturation water vapour pressure versus temperature, γ is the psychometric constant, Q^* is the net radiation at the surface computed using equation 3.17 and β a constant(20 Wm^{-2}) which has been introduced to compensate the deviation of near surface conditions from fully saturated air.

$$\boldsymbol{Q}^{*} = (1-0.23)K^{\downarrow} - C_S\frac{K^{\downarrow}}{K^{\downarrow}_{ext}} \dots\dots\dots\dots\dots\dots\dots\dots\dots\dots\dots\dots\dots\dots. (\mathbf{3.17})$$

Where $K^{\downarrow}$ is the daily downwelling short-wave radiation at the surface, $K^{\downarrow}_{ext}$ is the downwelling shortwave radiation constant at the top of the atmosphere, and C_S an empirical constant (110 Wm^{-2})

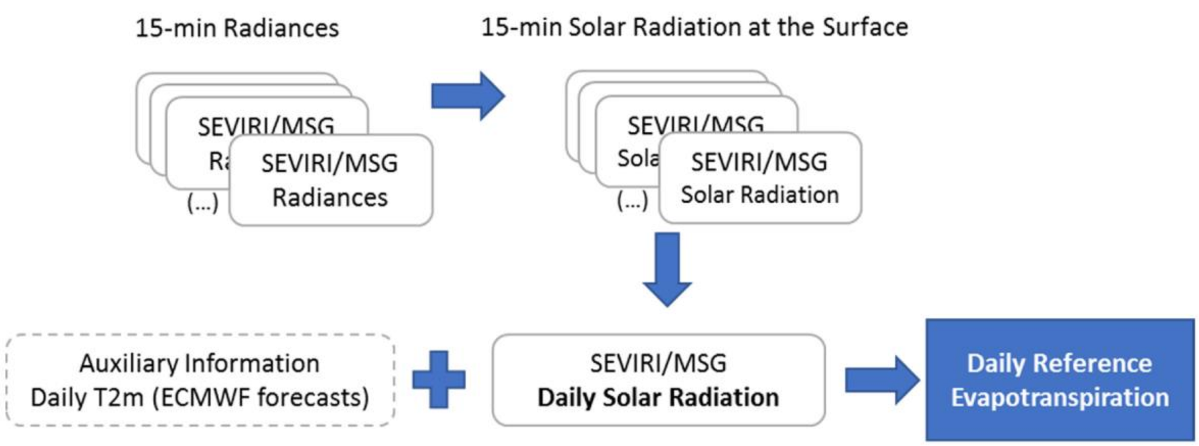

Figure 3-4: LSA SAF Reference Evapotranspiration inputs and processing steps (Trigo et al., 2018)

Trigo et al. (2018) compared DMETREF with commonly used methods of reference evapotranspiration estimation at diverse types of climate regime. The methods are Priestley-Taylor (Priestley & Taylor, 1972; McMahon et al., 2013), Makkink (De Bruin et al., 2010) and Penman-Monteith following the guidelines in FAO56 (Allen et al., 1998). In the first two methods, the net radiation is from LSA SAF Daily Downward Surface Shortwave Flux (DIDSSF) as input while in the third method, all estimates were obtained using uniquely in-situ measurements. Their comparison showed that the LSA SAF DMETREF and Makkink algorithm presented very similar agreement with the local measurements at Cabauw (The Netherlands), an area which is very close to the hypothetical FAO reference grass for conditions without advection. In conditions with no advection effect or local aridity, the Penman-Monteith FAO tends to overestimate the reference evapotranspiration observations. While in semi-arid area of the validating site with impact of local advection, Penman-Monteith FAO estimates found much closer to the observation.

The potential evapotranspiration and Penman-Monteith FAO reference evapotranspiration are found two confusing terms in literatures. For instance, Joo et al. (2018) and Tian et al. (2015) stated that the Penman-Monteith FAO method is used and recommended to estimate potential evapotranspiration for hydrological modeling in arid and semis arid area. However, McMahon et al. (2013) clearly explained the difference between potential evapotranspiration and Penman-Monteith FAO reference evapotranspiration and argued that Penman-Monteith FAO reference evapotranspiration is not recommended for hydrological modeling. Penman-Monteith FAO reference evapotranspiration has to be adapted to potential evapotranspiration to be used as input to hydrological modeling (McMahon et al., 2013; El-Zehairy, 2018).

The reference evapotranspiration computed from long term data of NMA calculated using the Penmann-Monteith and LSA SAF DMETREF is compared at dekadal time scale (Maathuis et al., 2018b). Their result shows that LSA SAF DMETREF has a reasonable correlation with a longer term mean in-situ based reference evapotranspiration. This study will validate LSA SAF DMETREF at daily time scale to the UTB. Reference evapotranspiration will be computed from weather station climatic variables using Penman-Monteith method (Allen et al. 1998). Similar to the satellite rainfall, LSA SAF DMETREF will be interpolated to 1km spatial resolution. Daily LSA SAF DMETREF values at each station will be extracted by crossing the in-situ observation points with corresponding pixel. The performance of LSA SAF DMTREF estimations will be evaluated at daily and seasonal time ranges. Then, LSA SAF METREF will be corrected for advection effect or local aridity as a function of near surface air temperature (Trigo et al., 2018) . All processing will be carried out using ILWIS software. The general methodology of potential evapotranspiration evaluation is shown in Figure 3-5. Then the daily potential evapotranspiration will be adopted multiplying daily corrected LSA SAF DMETREF by a coefficient of each land cover classes from Allen et al. (1998). During conversion to potential evapotranspiration, temporal variation of the coefficient will be considered (El-Zehairy, 2018).

The descriptive statistics in the rainfall evaluation will be also used to compare the satellite based reference evapotranspiration with the in-situ computed reference evapotranspiration.

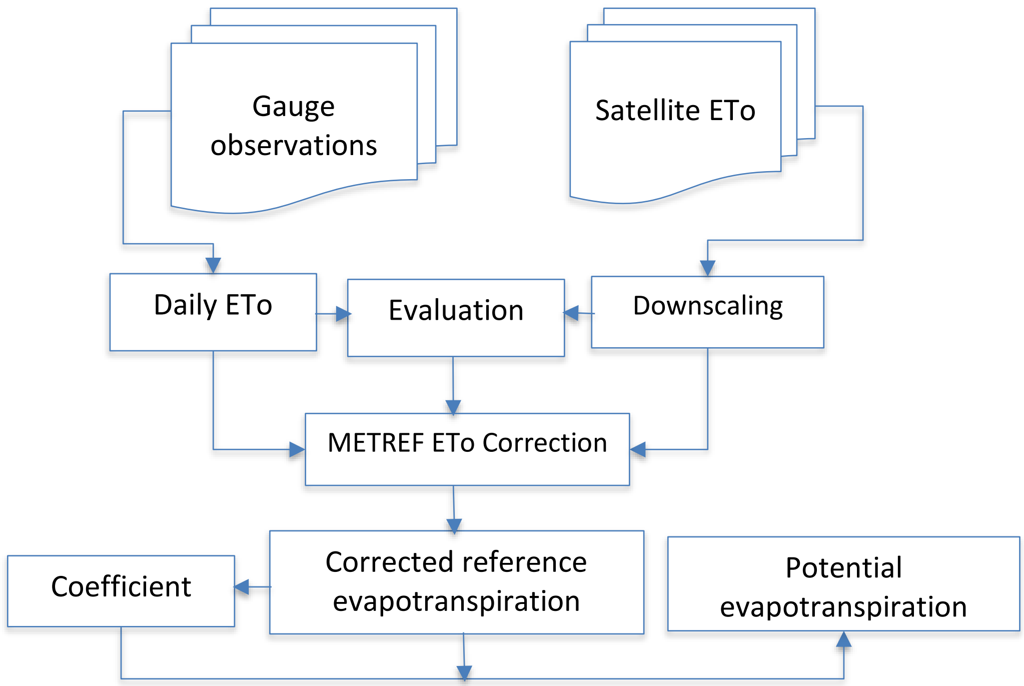

Figure 3-5: Flow chart of satellite reference evapotranspiration evaluation and conversion to potential evapotranspiration

4. Spatio-temporal variability of surface-groundwater interactions and groundwater resources -Objective-II

4.1. Introduction

Detailed water resource modeling is critically required for effective and sustainable water resources management. Integrated hydrological modeling requires significant understanding of the complexity of surface-groundwater interactions and are reliable methods to simultaneously simulate detail water flux such as evapotranspiration, runoff, recharge and discharge (Hassan et al., 2014). They can also be used to evaluate and predict surface-groundwater interaction in response LULC change impacts (Mateus et al., 2015). However, such studies have been simplified in arid and semi-arid environment (Teka, 2014; Barthel and Banzhaf, 2016; Sridhar et al., 2018; Feng et al., 2018b).

Water resources are the central elements for growth and transformation of Ethiopia (Melesse et al., 2013). The dependency on rainfed agriculture production system together with the progressive degradation of the natural resources and climate variability has aggravated the incidence of poverty and food insecurity in the country (Awulachew et al., 2007). As a result, groundwater is the alternative resource to supplement surface water resources for small irrigation and for domestic and industrial water use especially in rural areas and towns (Melesse et al., 2013; Worqlul et al., 2017). However, spatio-temporal surface-ground water interaction in response to the dynamic LULC, particularly in semi-arid UTB, is not well known. According to Kebede et al. (2005) the total annual recharge in Tekeze Basin differs from report to report and it is more general. Such conventional way of groundwater resources studies of storage may mislead to poor water resource management and failure of plans. To the knowledge of the researcher, there are no studies conducted in the study area on surface-groundwater interaction using integrated hydrological model. Therefore, an integrated hydrological model will be conceptualized and calibrated to quantify spatio-temporal water fluxes in semi-arid UTB of northern Ethiopia which could helpful for decision makers to improve sustainable water resource management.

4.2. Data acquisition

In-situ data and remote sensing data will be sourced as input to integrated hydrological modeling.

In-situ data

This study will employ both primary and secondary datasets from field measurements, databases and observations. Due to the growing demand of water resources, monitoring the surface and groundwater levels are important as state variable for model calibration and as baseline document for water resource change evaluation temporally and spatially. River discharge for the outlet of study area will be sourced from Ministry of Water Irrigation and Energy of Ethiopia. At information level, this instrument is recording since 2015 at 15 minute time interval. Four additional automatic data loggers for river discharge measurements will be installed in the main streams above the outlet of the catchment. Suitable area for installation of these instruments will be decided after field work observation. Automatic groundwater level measuring data loggers will be also installed which will be used for calibrating the integrated hydrological model. The installation of the groundwater level loggers will be in accordance to the hydrogeological characteristics and existing well distribution. The river data loggers will be programmed for 10 minute interval while groundwater level loggers for 1 hour interval. The monitoring period for both river and groundwater data loggers will be for 2 years. Soil data will be sourced from the Ethiopian Soil Information System (EthioSIS). Topographic map will be also sourced from Ethiopian Geospatial Information Agency for locating reference elevation points. The reference points will be used to measure the surface elevation above mean sea level using differential global positioning system (DGPS). This survey will be used to determine the accurate hydraulic heads through groundwater level measured from the surface by deducting the casing height and concrete slabs in the wells. Geology and hydrogeology maps will be sourced from the Geological Survey of Ethiopia to develop a conceptual model and for parameterization of the numerical model. Borehole information and hydrogeological reports will be collected from Tigray regional water resource office and other water enterprises. All data sets will be checked and re-projected/georeferenced to consistence coordinate system.

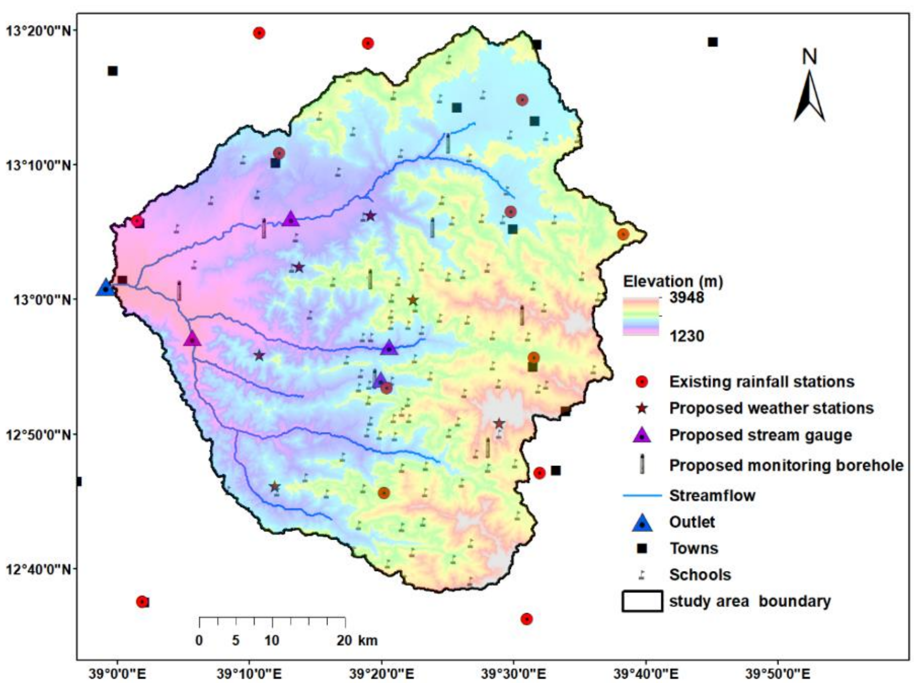

Figure 4-1: Proposed monitoring boreholes, streamflow gauging and weather stations

Remote sensing data

Satellite rainfall and potential evapotranspiration as driving force to integrated hydrological models will be selected after validation and integrated with in-situ observations. Shuttle Radar Topography Mission (SRTM) digital elevation (DEM) digital elevation model (DEM) with 30-m resolution will be used to define the study area and topographical attributes. Sentinel-2 satellite image will be used to classify the LULC of the study area. This satellite image will be downloaded free of charge from the United States Geological Survey (USGS) via http://earthexplorer.usgs.gov/. Seasonal normalized difference vegetation index (NDVI) will be calculated from the Sentinel-2 satellite image to compute the vegetation density (percentage of green over each hydrologic response unit). The vegetation density will be used to parameterize the surface hydrological model.

4.3. Methodology

4.3.1. Conceptual model

Distributed numerical groundwater models are playing a key role in evaluating the groundwater resources and management. The pre-requisite to develop such model is developing conceptual models (Lekula et al., 2018). A conceptual model is a qualitative representation of a groundwater system with a minimum information on boundaries; hydrostratigraphy and hydrogeologic properties; flow directions and sources and sinks; and a field-based estimate of components of the groundwater budget (Anderson et al., 2015).

Boundary conditions and flow direction

Boundary condition are the main component of numerical modeling that strongly influence the flow directions calculated by the model (Anderson et al., 2015). These may include groundwater divides, water bodies, impermeable rock and rivers. Accordingly, the boundary conditions for this study will be defined to represent the groundwater flow moving in or out of the study area boundary. The Eastern boundary of the study area will be assumed as water divide because this boundary is a watershed divide with high elevation that divides the eastern and western area and the drain networks are directed to the west. The northern and western boundaries are also parallel to the stream flows (Figure 4-2). Moreover, Girmay et al. (2015) generalized that groundwater contour maps in part of Upper Tekeze River Basin are similar to the topographic contours indicating the groundwater flow is similar to the surface flow direction. Therefore, a no-flow boundary condition is proposed to the groundwater flow except the outflow in the West outlet of the study area (Figure 4-2). However, the boundary conditions may be re-adjusted after fieldwork observation and collection of all required information. All relevant hydrogeological data will be organized and analyzed using geographic information system tools during developing the conceptual model. Static water level of boreholes will also be verified at national and regional level. Then hydraulic head from boreholes will be computed by deducting the static water level from the surface elevation. The point wise hydraulic head will be interpolated using kriging with external drift. This method will be applied because of its ability to improve both the precision and realism spatial hydraulic heads (Rivest et al., 2008). DEM will be used as explanatory variable during interpolation of the hydraulic head.

Springs are common in the UTB particularly on volcanic rocks and their significant discharge suggest the productivity of aquifer in the UTB (Girmay et al., 2015). In this study, the characteristics of springs will be analyzed to understand how they behave in space and time and their representation to the groundwater table depth will be also investigated.

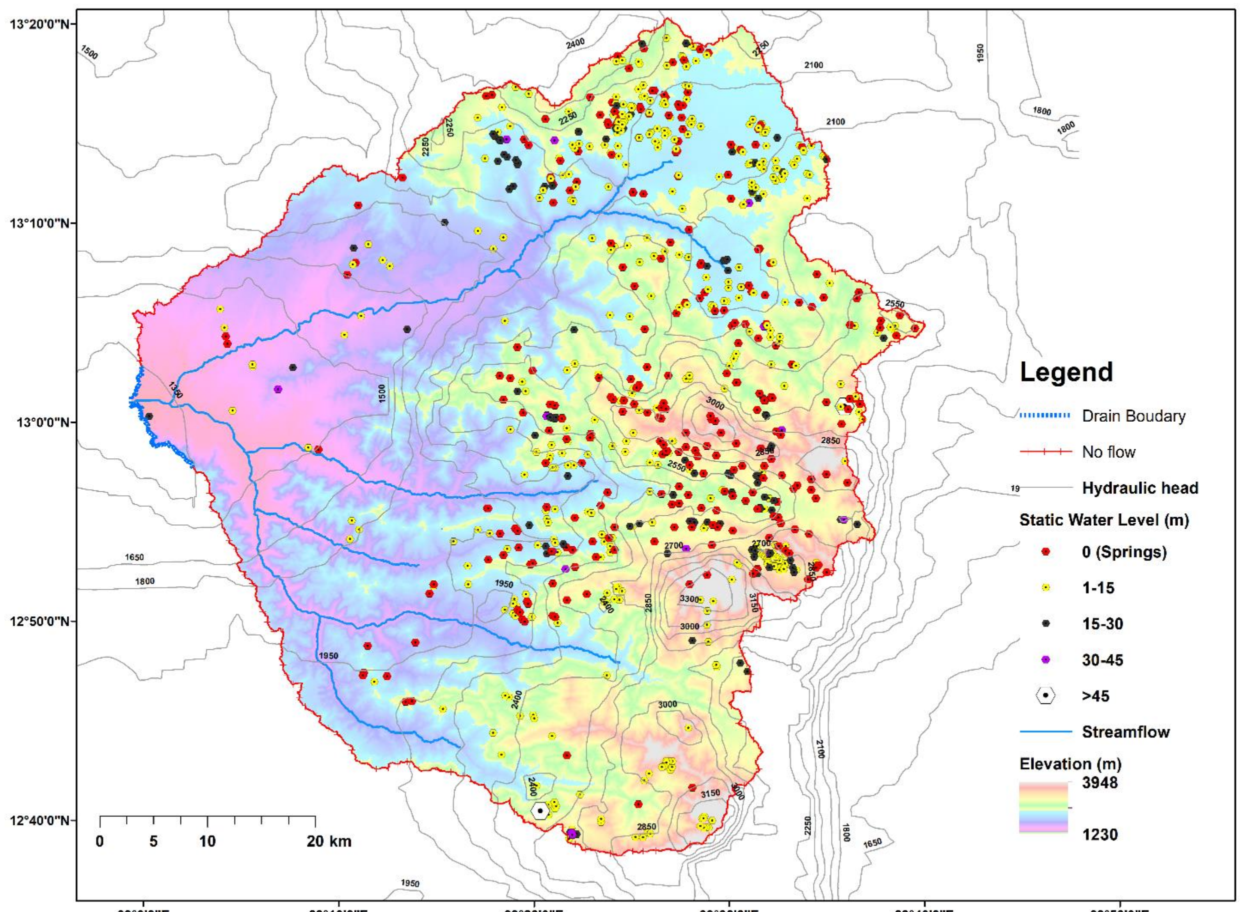

Figure 4-2: Hydraulic head contours and proposed boundary condition

Hydrostratigraphic units

Hydrostratigraphic units depends on the hydrogeological formations of layers. The geologic formation of the study area is mainly characterized by volcanic at the upper most, sand stone and limestone in the middle and meta volcanic as basements. There are no data at this stage to define the Hydrostratigraphic units of the study area and a geology and aquifer characterization is also proposed as part of this study. Therefore, the vertical layer will be defined based on lithological features and hydrogeological characteristics. According to three borehole information, the unconsolidated material in the north west is with thickness ranging between 2 to 26m in limestone and shale lithology. Two boreholes log information in the north east also show that the unconsolidated material is with thickness up to 9m. However, these data are not representative to define the hydro-stratigraphic units of the study area. For this stage, two layers are proposed: the upper unconsolidated as unconfined aquifer and composed limestone and sandstone as confined aquifer. This will be refined and may be changed after detail analysis of borehole information and geological formations

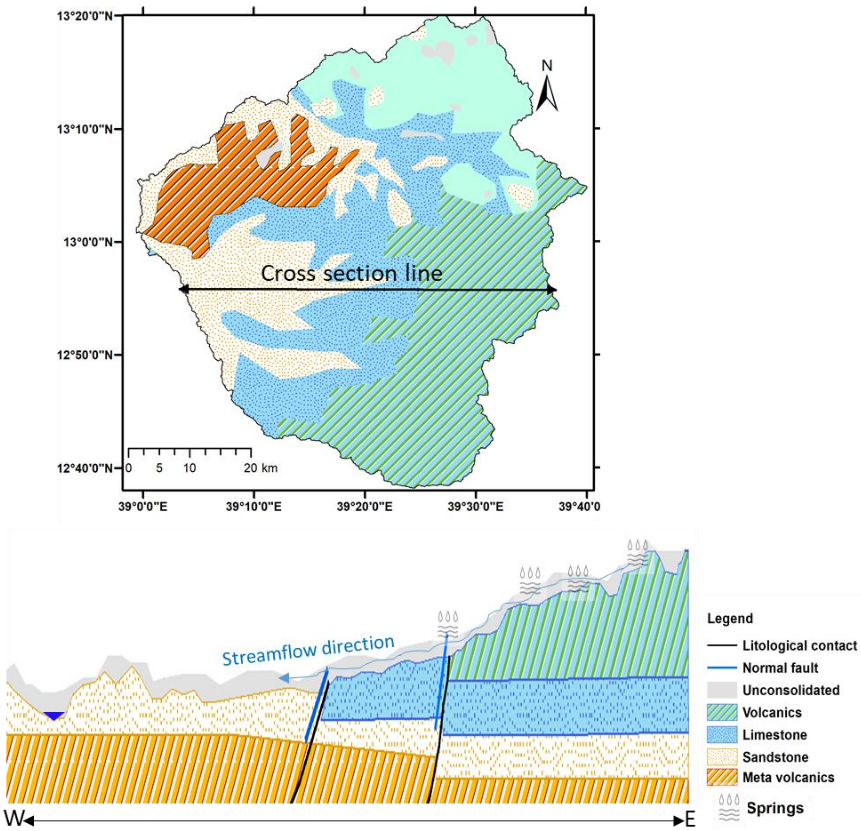

Figure 4-3: General geological cross section from study area (processed from Geological Survey of Ethiopia)

Preliminary water balance

Constructing the preliminary water balance in conceptual model is important to identify the important water balance components to be considered and how they interact. In the study area, rainfall is the only source of water to the system. The rainfall is partly intercepted by plants and the remaining rainfall as effective rainfall that will be distributed in to different components of hydrologic processes. The main outputs are the evapotranspiration and outflow towards to the western discharge.

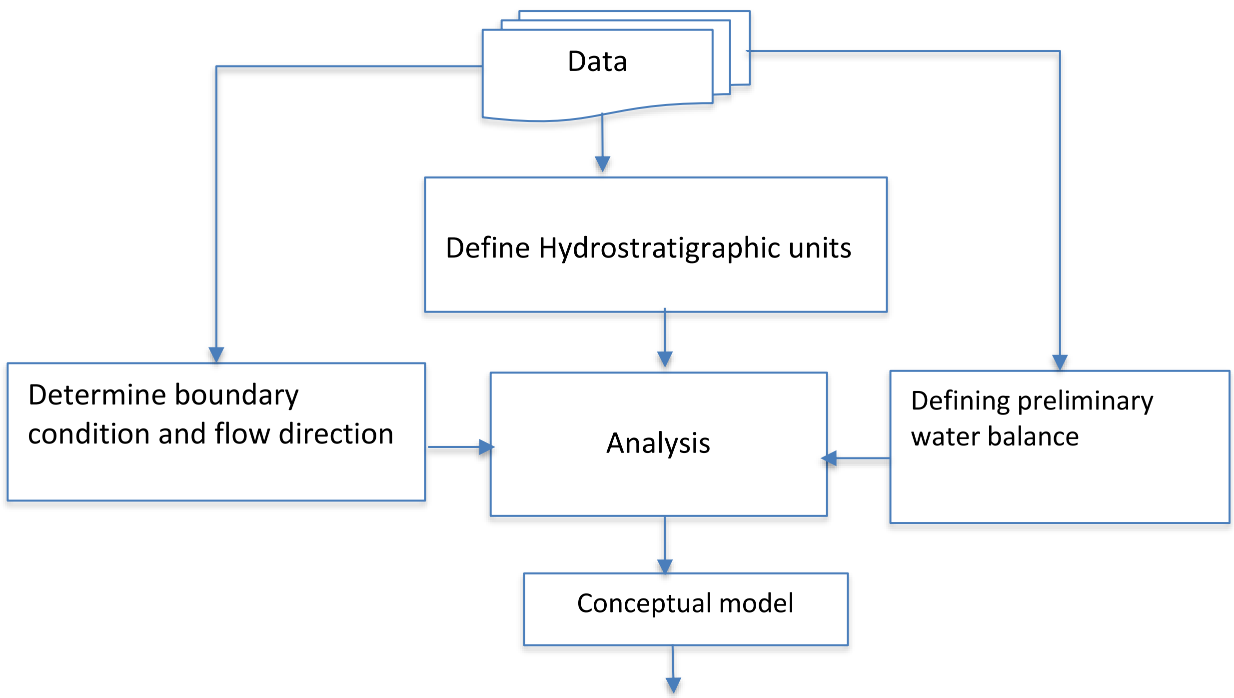

Figure 4-4: General methodology to develop hydrological conceptual model

4.3.2. Integrated hydrological model selection

Integrated hydrological models are crucial in addressing complex water cycle interactions and management issues. As a result, different models have been developed; example, HydroGeoSphere (Brunner & Simmons, 2012), MIKE-SHE (Graham & Butts, 2005), ParFlow (Vanderkwaak & Loague, 2001), CATHY (Camporese et al., 2010) and GSFLOW (Markstrom et al., 2008). However, the initial applications of integrated hydrological model have been limited to small catchments (Sebben et al., 2013). In the recent years, these models are becoming the robust tools that provides spatial and temporal details of water resources system at regional scale but the large amount of data required to parameterize and evaluate the models is still challenging (Sebben et al., 2013). The performance of these models is also subjected to uncertainty because of their complexity (Wu et al., 2014). Therefore, selecting integrated hydrological model considering its complexity, data requirement and data availability is important.

This study will apply coupled Groundwater and Surface-water FLOW (GSFLOW) model. GSFLOW was developed to simulate coupled groundwater-surface-water flow across the land surface and within subsurface saturated and unsaturated materials (Markstrom et al., 2008). GSFLOW model comprehensively reproduces water fluxes with high spatial and temporal resolutions and can be used to evaluate surface and subsurface flow responses to land use change, climate variability, and ground-water withdrawals (Hassan et al., 2014; Wu et al., 2015; Fulton et al., 2015). GSFLOW is better to estimate the spatial and temporal variability of evapotranspiration, infiltration, recharge, ground-water discharge, and stream flow generation (Markstrom et al., 2008). GSFLOW reproduces all major processes of the terrestrial water cycle by comprising three modules (Feng et al., 2018b): 1) a surface module for simulating surface water and root zone soil water 2) a subsurface module for modeling vadose zone flow and groundwater flow 3) a stream-lake module that routes water through surface water bodies. GSFLOW introduces the concept of a gravity reservoir that enables water flux between surface and groundwater interaction. Therefore, this model is selected because of its ability to simulate flow across the land surface, within saturated and unsaturated subsurface materials; can be applied in single or multiple watersheds with different area coverage; suitable to apply in time periods ranging from months to decades (Markstrom et al., 2008). Moreover, GSFLOW model is also suitable in mountainous regions where mostly the rainfall is high which is also true in this study.

4.3.3. Model setup

GSFLOW works based on the integration of the USGS Rainfall-Runoff Modeling System (PRMS) and the USGS Modular Groundwater Flow Model (MODFLOW) to simulate coupled surface water and groundwater resources (Markstrom et al., 2008; Ely and Kahle, 2012). In GSFLOW, the surface domain can be delineated into hydrologic response units (HRUs) and the subsurface domain can be defined vertically into multiple layers based on hydrogeological information and horizontally discretized into finite difference grids.

PRMS discretized catchment into a network of HRUs based on hydrologic and physical characteristics of the catchment (Markstrom et al., 2008). Modified GSFLOW model setup by Hassan et al. (2014) will be adopted to simulate the hydrological responses by PRMS and MODFLOW-NWT (Figure 4-5). The GSFLOW with Newton solution version method is suitable for this study because of its ability to solve problems involving drying and rewetting in hydrogeologic settings which are dominated by nonlinearity. Moreover, this feature is particularly important to study areas characterized by unconfined conditions, steep topography and surface-groundwater interactions (Fulton et al., 2015) which represent this study area.

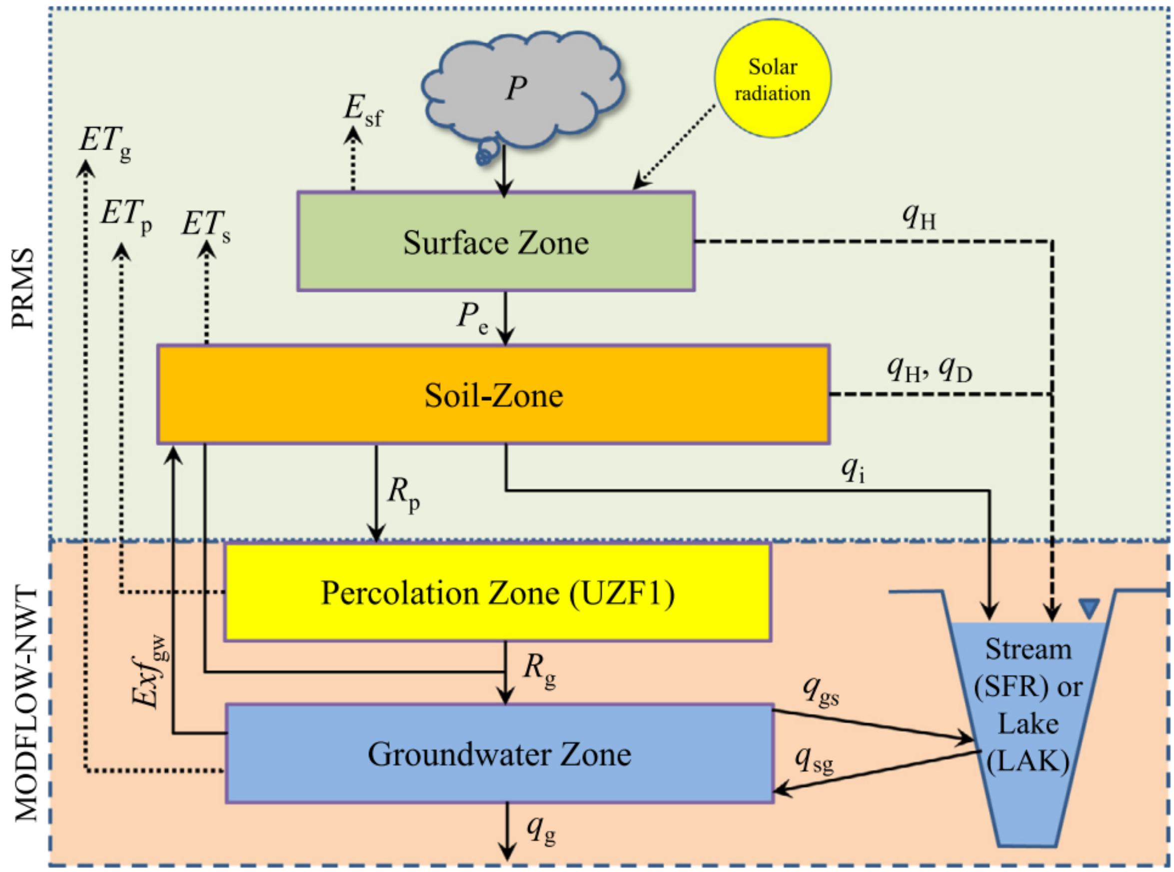

Figure 4-5: Schematic diagram of GSFLOW setup (Hassan et al., 2014)

where: P -rainfall; E_{sf} - evaporation of intercepted rainfall and evaporation from impervious areas; ETs- evapotranspiration from the soil zone; ET_p- evapotranspiration from percolation zone; ET_g- groundwater evapotranspiration; P_e- rainfall excess infiltration; R_p-percolation beneath the soil zone; R_g-gross recharge; q_H - Hortonian overland flow to streams; q_D- Dunnian saturation excess runoff to streams (or lakes); q_i - interflow; q_{gs}- groundwater discharge to streams (or lakes); q_{sg}-stream discharge to groundwater; q_g - lateral groundwater outflow (sink term); Exf_{gw}- groundwater exfiltration to soil zone.

The catchment boundary and stream networks for this study will be processed from DEM. The surface model domain delineation into HRUs will be performed using ArcHydro extension of ArcGIS. The sub-surface domain will be discretized in to grid cells with 1×1 km cell size horizontally, similar to the spatial resolution of rainfall and potential evapotranspiration, using ModelMuse. The conceptual model will be converted to numerical model here. The sub-surface parametrization will be performed based the topographical, geology and soil zonation to facilitate the trial and error parameterization. Moreover, parameters estimated in borehole data or existing reports and ranges of parameters from literature will be considered.

This study is open to use the newly released MODFLOW-USG (UnStructured Grid version of MODFLOW) of MODFLOW 6 combining unstructured grid option too. MODFLOW-USG discretization provides flexibility of MODFLOW domain using different shaped geometries individually or in combination in contrast to the traditional MODFLOW which uses structured grids (Panday et al., 2013). The MODFLOW-USG is flexible in grid design to focus resolution on interest of area or to sub-discretize individual layers to better represent hydrostratigraphic units. However, this method is out of scope in this proposal stage for detail presentation.

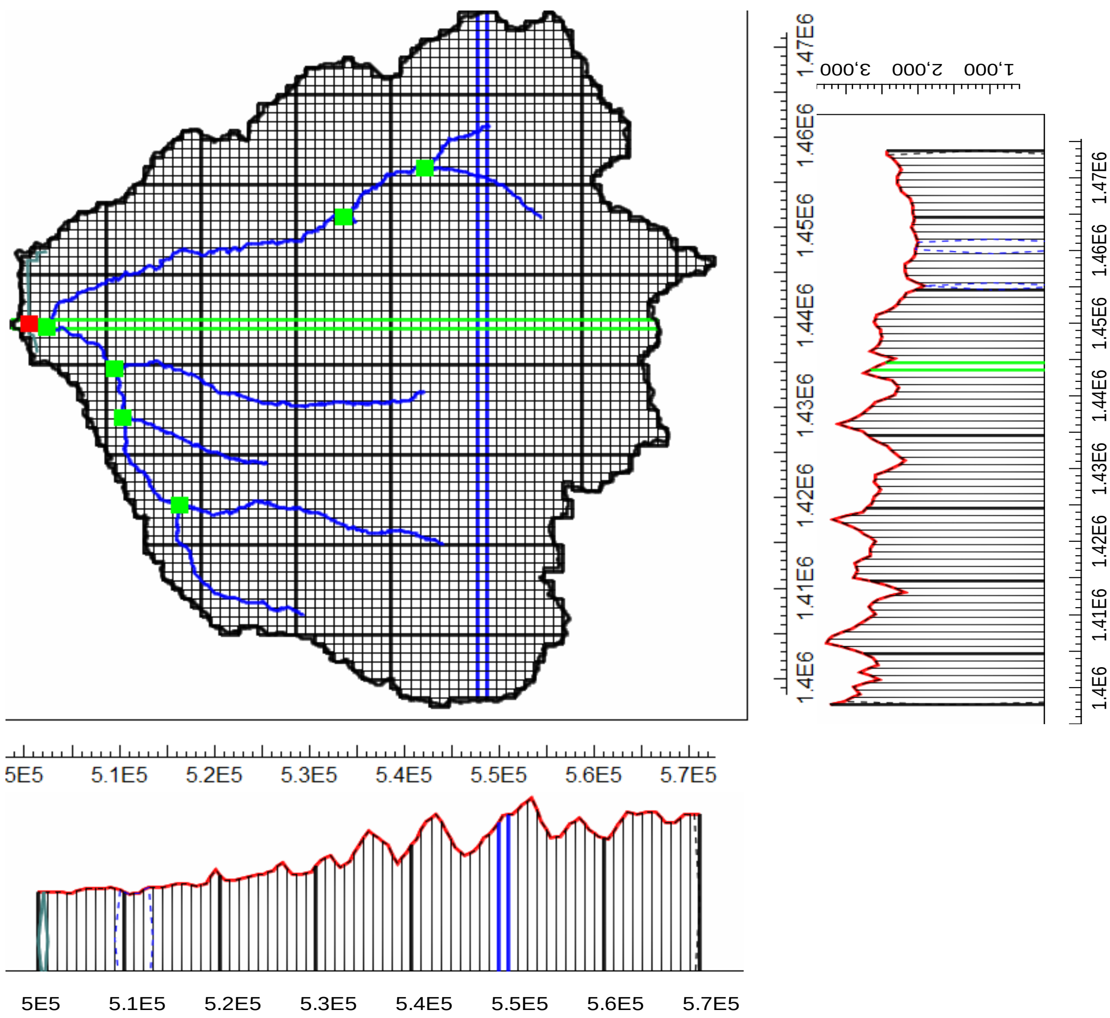

Figure 4-6: topographic cross section at 1km resolution of East-West (front side) and North-South (side)

4.3.4. Model input preparation

The GSFLOW data input consists of the inputs for PRMS and MODFLOW-NT. The PRMS consists of climate inputs, land surface and soil. Spatially distributed parameters related to soil such as available water holding capacity of the soil, each texture content of soil and soil depth to bed rock will be prepared from soil map attributes. Vegetation density will be prepared from the NDVI of LULC using vegetation fraction method (Zhou et al., 2015). Then parameters of each HRUs will be initially estimated from DEM, land use type, soil data, and vegetation data which will be further adjusted during model calibration. Preparation and estimation of these parameters will be performed in ArcGIS environment.

Control file and parameter file are as part of input files in the PRMS model. The control file contains all control parameters related to model execution, input, output, specification of the active modules. The parameter file defines required parameters with their dimensions for simulation. Therefore, USGS PRMS Paramtool will be used to prepare the PRMS parameter and control file formats.

Daily grid rainfall and potential evapotranspiration as inputs to the GSFLOW from side of MODFLOW-NWT will be prepared to the same extent and coordinate system. These grid files will be converted to the format compatible as input to ModelMuse. In the rainfall input, the interception will be considered because interception play as a significant loss by increasing evaporation and decreasing the amount of water available for infiltration particularly in semi-arid areas (Li et al., 2016). Considering this loss, temporally and spatially variable interception rate maps appropriate for semi-arid areas will be prepared at the model grid resolution. A function will be used in ModelMuse to convert the corrected satellite rainfall into spatio-temporally variable effective rainfall. The daily potential evapotranspiration will be prepared by multiplying daily LSA SAF DMETREF with the spatially and temporally variable coefficients maps of each LULC classes.

4.3.5. Model calibration

The three step model development approach by Fulton et al. (2015) will be adopted for this study because this approach can improve prediction performance of the model. First, develop and calibrate PRMS model. Secondly, develop and calibrate the steady state MODFLOW-NWT model. Thirdly, the PRMS and MODFLOW-NWT models will be integrated in to the GSFLOW structure and calibrate the GSFLOW using the individually calibrated PRMS and MODFLOW-NWT models as a starting point. Stepwise trial and error calibration approach will be applied to this study at daily time step from 2015 to 2021. Trial and error calibration method is advantageous because a modeler can incorporate subjective knowledge and gain understanding about the model behavior during the calibration process (Hassan et al., 2014). Then daily stream flow and groundwater heads will be used calibrate GSFLOW model.

Model performance related to hydraulic heads and discharge will be evaluated using graphical comparison and statistical descriptions of RMSE and NSE (Eq.16 and Eq.17). The NSE describes the overall accuracy of model simulations in hydrological modelling (Nash & Sutcliffe, 1970). Calibration will be done iteratively until no improvement by RMSE and NSE objective functions.

Sensitivity analysis plays important roles in model parameterization, calibration, optimization, and uncertainty quantification (Song et al., 2015). Hence, the sensitivity of water fluxes to parameters of GSFLOW model will be performed and sensitive parameters will be selected and presented.

$$RMSE = \sqrt{\frac{1}{T}\sum_{i=1}^{T}\left(Obs_i - Sim_i\right)^2} \tag{4.1}$$

$$NSE = 1 - \frac{\sum_{i=1}^{T}\left(Sim_i - Obs_i\right)^2}{\sum_{i=1}^{T}\left(Obs_i - \overline{Obs}\right)^2} \tag{4.2}$$

Where Obs_i is observed stream flow/groundwater heads; Sim_i is model simulated stream flow/groundwater heads; the over bar Obs_i represents for average of observed stream flow/groundwater head levels; T is the total number of simulated and observed data pairs (days).

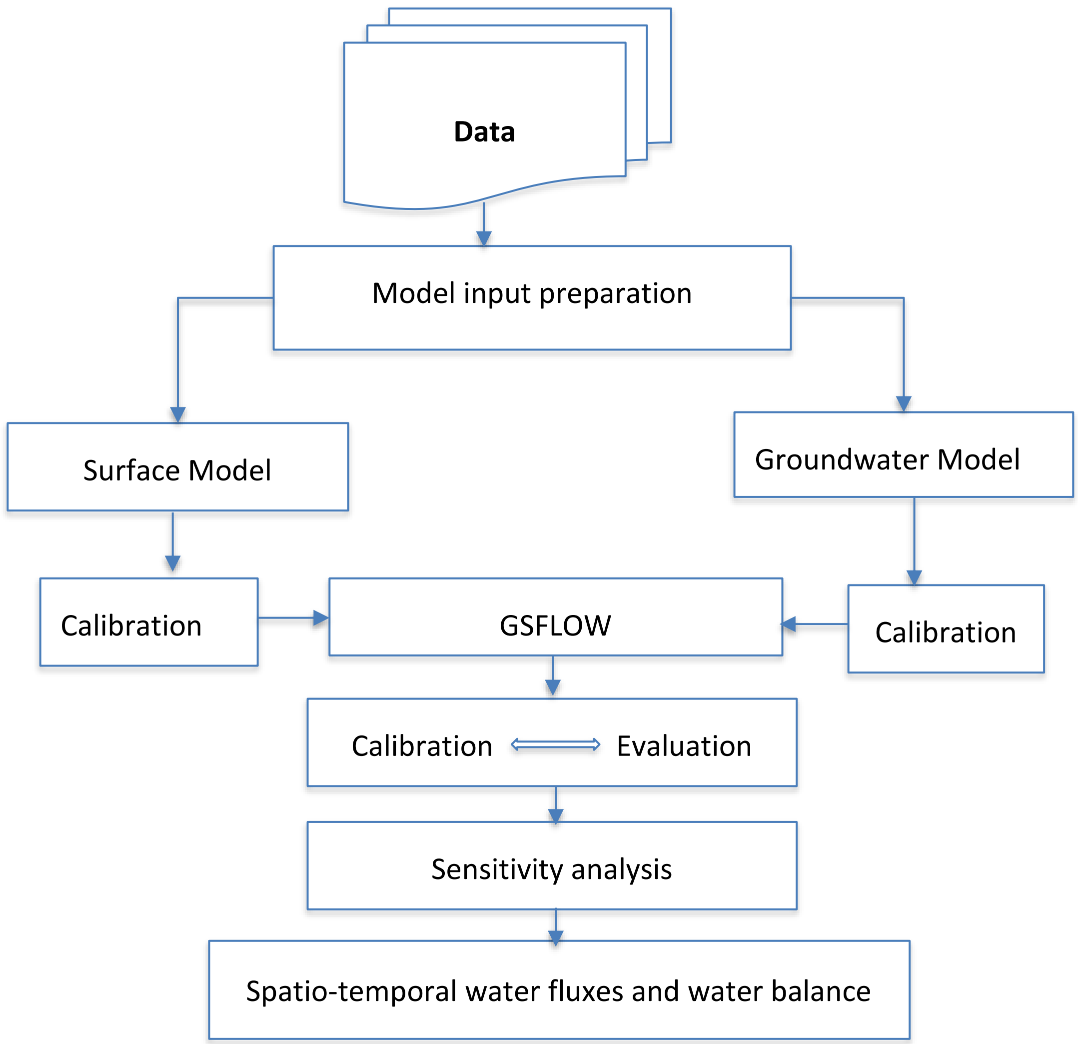

Figure 4-7: General flowchart of GSFLOW modeling methodology

5. Predict future water resources changes in response to future LULC change-Objective-III

5.1. Introduction

LULC change is among the consequence of human induced global environmental change affecting groundwater recharge (Zomlot et al., 2017) by affecting the hydrological flow pathways (Zwartendijk, 2015). The evaluation of LULC effects on groundwater recharge model parameters by Jinno et al. (2009) showed that LULC significantly affect groundwater recharge and discharge and surface water flows by altering infiltration rate. LULC change impact on recharge dynamics and vadose zone will be also continuing globally (Kim & Jackson, 2012). LULC change has a significant impact on both magnitude and pattern of surface runoff, groundwater and soil moisture content (Davis et al., 2015; Setyorini et al., 2017). Therefore, predicting future LULC change impact on groundwater storage helps to identify the future potential consequences and as a base for integrated water resource management and adaptation (Schaldach et al., 2011; Hoyer & Chang, 2014; Grinblat et al., 2015; Pulido-Velazquez et al., 2015). Evaluating LULC change impact on water resources is more valued in arid and semi-arid area where more people rely on groundwater during dry season like Ethiopia. Most Ethiopian population is engaged in rainfed agriculture with very small proportion of water for irrigation from surface water. More than 90% of the water used for domestic and industrial supply in Ethiopia is provided from groundwater (Kebede et al., 2018). Therefore, studying the dynamic LULC change impact on the surface and groundwater resources and their interaction is crucial. However, many of the researches in Ethiopia focused on the scale of LULC change missing its impact on surface-groundwater interaction (Melesse & Abtew, 2015). A study by Welde & Gebremariam (2017) showed significant dynamic LULC change transitions with significant impact on the hydrology of Tekeze dam Catchment. However, the impact of future LULC changes on surface-groundwater resources is not studied though intensified agriculture expansion is foreseen in the study area.

There are many driving factor variables that potentially influence LULC dynamics (Keshtkar & Voigt, 2016). These factors are the predictors for LULC distributions. For example Zhen et al. (2014) and Samie et al. (2017) grouped different factors in to four main categories: geophysical; climatic; proximity; and socioeconomic. The population growth and associated demand for land are the major driving forces for LULC changes which is also affecting the water resource (Haregeweyn et al., 2015). LULC changes can be predicted in consideration of these factors using spatially explicit LULC change models which are robust tools to predict its dynamics (Takahashi et al., 2004; Zhen et al., 2014;Ghosh et al., 2017; Samie et al., 2017). Along the spatially explicit LULC change models, geospatial technology, particularly the remote sensing and geographic information system (GIS), based predictions of LULC provide quantifiable spatial changes for LULC classes (Weng, 2002).

Therefore, this study will predict future water resources in response to future LULC change scenarios. Understanding the water resources responses to future LULC change can help decision makers for sustainable water resource and LULC change management.

5.2. Data acquisition

Sentinel-2 and Landsat satellite images to be used for LULC classification will be sourced from United States Geological Survey (USGS) via http://earthexplorer.usgs.gov/. Moreover factors that affect LULC will be calleted from respective organizations.

5.3. Methodology

Landsat Thematic Mapper images for 1990, 200, Landsat 8 and Sentinel-2 for 2018 time periods will be used to classify the LULC of UTB. The Sentinel-2 image will be resampled to the resolution of Landsat image and compared with Landsat 8 to be consistent with the past Landsat images. The LULC change will be produced following appropriate LULC classification system. Preprocessing tasks such as radiometric and geometric corrections will be checked and corrected. Ground control points (GCPs) will be collected during field work for image classification and accuracy assessment. Then supervised classification will be used to produce the 2018 LULC classes. Then accuracy assessment will be performed with independent GCPs that are not used in the image classification. Information local elders and Google Earth images will be also undertaken to classify and assess the accuracy of images in 1990 and 2000. ERDAS Imagine and ArcGIS applications will be used during image processing activities.

5.3.1. LULC prediction

The future LULC patterns will be projected using a dynamic and spatially explicit model. There are many LULC change models with their strong side and limitation (Gidey et al., 2017) though there is no clearly prioritized approach to model LULC changes (Takahashi et al., 2004). However, the Markov Chain and Cellular Automata Analysis (CA-Markov) model, a hybrid of the cellular automata and Markov models, is the most commonly used spatially explicit model in recent literature because of its consideration to the spatial and temporal components of LULC dynamic (Behera et al., 2012; Zhen et al., 2014;Keshtkar & Voigt, 2016; Gashaw et al., 2017; Ghosh et al., 2017; Gidey et al., 2017; Hyandye & Martz, 2017;Samie et al., 2017). Therefore, this study proposed to use the CA-Markov model to predict LULC change for the study area for 2035 time period.

CA-Markov basically requires three types of data inputs to predict LULC change predication (Hyandye & Martz, 2017). These are the basis temporal LULC image, Markov transition areas file and transition suitability images collection. Basis temporal LULC are prepared following the satellite image classification. The Markov transition areas files are generated by running a Markov module prior to executing a CA-Markov module during the implementation of the Markovian LULC change modelling. The LULC transition suitability maps are prepared by aggregating a collection of maps (factors and constraints) using the multi-criteria evaluation (MCE) method. Factors are criteria that define some degree of suitability for all geographic regions while constraints are those Boolean criteria that limit analysis to a particular geographic regions (Eastman, 2012).

The factors affecting the LULC of the study area will be identified and weighted using local elders' knowledge and experts (Gashaw et al., 2017; Gidey et al., 2017). Researcher's point of view factors might be included after field observation and discussion with experts. The constraints in this study will be applied to the scenarios on LULC related polices in Ethiopia. All identified factors and constrains will be prepared in ArcGIS environment which will be used as input the LULC dynamic model. Then the weight of each LULC factors will be determined using pairwise comparison in the Analytical Hierarchy Process (AHP).

A transition probabilities for the years 1990-2000 and 2000-2018 will be obtained based on the CA-Markov approach. Then LULC for the year 2018 will simulated using the transition probabilities from 1990 to 2000 with baseline LULC of 2000 and this will be used as model validation by comparing the simulated with the classified LULC of 2018. Finally, the LULC for 2035 will be projected using the transition probabilities from 2000 to 2018 and the LULC base map from the year 2018 under given scenarios. The scenarios Business as Usual (BAU) and Forest Conservation and Water Protection (FCWP) by Welde & Gebremariam (2017) will be adopted during prediction of the future LULC change. These scenarios are selected because they are based on the existing LULC related polices in Ethiopia. Based on these scenarios, future LULC changes will be generated.

Then the validated and calibrated GSFLOW will be run based on the future LULC scenarios. Quantitative and qualitative analysis will be performed on the future water resources of the catchment in response to future LULC change. Then water fluxes and detail water balance changes of the current and future periods will be analyzed to answer how the catchment is sensitive to future LULC change.

Table 5-1: LULC scenarios and assumptions (Kindu et al., 2018)

Scenario	Assumption
BAU	*Continuation of historical LULC changes*
FCWP	*Strict implementation of spatial policies: no change allowed with in natural forests, plantation forests, woodlands and water bodies*

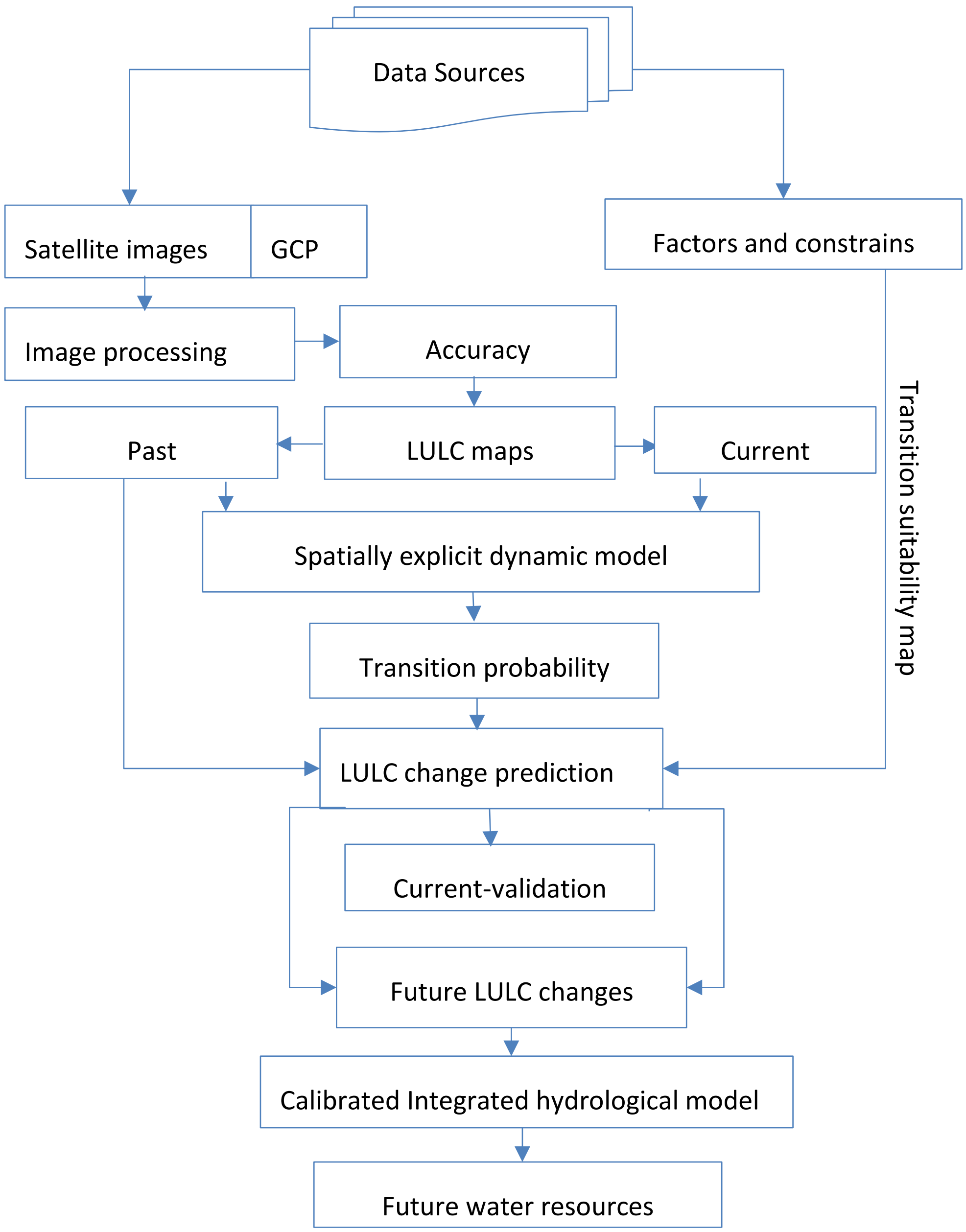

Figure 5-1 General flowchart of methodology for future water resources modeling

6. Expected outputs

Understanding the water resource responses of semi-arid upper Tekeze basin to LULC is an important component of water resource management. Therefore, predicting changes of water resource that would likely exist in the future helps to make proper planning for sustainable water resources in line with the ambitious plan for intensive agricultural practices. This study can contribute as a pilot study to undertake similar studies in other Basins. Moreover, this study will help to decision makers on formulating sound policy, strategies and the public better understand and manage the water resources in the Basin in a sustainable manner. This study will contribute to the following major research outputs:

- Integrated hydrological model that can be scaled to other catchments or scarcely gauged basins (e.g. those in the direct neighborhood of the Tekeze Basin such as Tana and Beshelo)
- Quantified water fluxes and detailed water balance of the study area
- Four published papers in peer reviewed journals
    - I. Validating and improving satellite rainfall in UTB
    - II. Spatio-temporal variability of potential evapotranspiration in UTB
    - III. Assessment of surface-groundwater interaction in data scarce environment using integrated hydrological modelling approach in UTB
    - IV. Water resources changes under future land use land cover changes in UTB

MSc Topics

- Land use land cover dynamics and catchment characterization of UTB
- Geology and aquifer characteristics of UTB

7. Work plan

No	Activities	2018						2019												2020												2021												2022						
		J	A	S	O	N	D	J	F	M	A	M	J	J	A	S	O	N	D	J	F	M	A	M	J	J	A	S	O	N	D	J	F	M	A	M	J	J	A	S	O	N	D	J	F	M	A	M	J	J
1	**Literature review**																																																	
2	**Proposal development**																																																	
3	**Progress report**																																																	
4	**Seminars and workshopes**																																																	
5	**Course work**																																																	
6	**Fieldwork and data collection**																																																	
7	**MSc students supervision**																																																	
8	**Satellite rainfall and potential evapotranspiration analysis**																																																	
9	**Hydro-geological conceptual model development**																																																	
10	**Integrated hydrological modeling developemnt**																																																	
11	**LULC change analysis and prediction**																																																	
12	**Result analysis and writeup**																																																	
	i. Validating and improving satellite rainfall and potential evapotranspiration																																																	
	ii. Hydro-geological conceptual model																																																	
	iii. Surface-groundwater interaction in data scarce environment using integrated hydrological modelling																																																	
	iv. Water resources changes under futre LULC changes																																																	
13	**Manuscript preparation and send to Journal publication**																																																	
	i. Validating and improving satellite rainfall																																																	
	ii. Spatio-temporal variability of potential evapotranspiration in UTB																																																	
	iii. Assessment of surface-groundwater interaction in data scarce environment using integrated hydrological modelling approach in UTB																																																	
	iv. Water resources changes under future land use land cover changesLULC changes																																																	
14	Thesis submission																																																	

Key:
- ITC,UT
- MU, Ethiopia
- ITC and MU

References

Alazzy, A. A., Lü, H., Chen, R., Ali, A. B., Zhu, Y., & Su, J. (2017). Evaluation of Satellite Precipitation Products and Their Potential Influence on Hydrological Modeling over the Ganzi River Basin of the Tibetan Plateau. *Advances in Meteorology*, *2017*. https://doi.org/10.1155/2017/3695285

Alemayehu, T. (2006). Groundwater occurrence in Ethiopia. Addis Ababa University Press, Addis Ababa, pp 1–105.

Allen, R. G., Luis, S. P., RAES, D., & Smith, M. (1998). FAO Irrigation and Drainage Paper No. 56. Crop Evapotranspiration (guidelines for computing crop water requirements). *Irrigation and Drainage*, *300*(56), 300. https://doi.org/10.1016/j.eja.2010.12.001

Anderson, M.P., Woessner, W.W., Hunt, R. J. (2015). Applied Groundwater Modeling : Simulation of Flow and Advective Transport,2 ed. Elsevier Science, San Diego.

Awulachew, S. B., Yilma, A. D., Loulseged, M., Loiskandl, W., Ayana, M., & Alamirew, T. (2007). *Water resources and irrigation development in Ethiopia*. *Colombo. International Water Management Institute (working paper 123)*. https://doi.org/10.1017/CBO9781107415324.004

Ayehu, G. T., Tadesse, T., Gessesse, B., & Dinku, T. (2018). Validation of new satellite rainfall products over the Upper Blue Nile Basin, Ethiopia. *Atmospheric Measurement Techniques*, *11*(4), 1921–1936. https://doi.org/10.5194/amt-11-1921-2018

Bai, P., Liu, X., Yang, T., Li, F., Liang, K., Hu, S., & Liu, C. (2016). Assessment of the Influences of Different Potential Evapotranspiration Inputs on the Performance of Monthly Hydrological Models under Different Climatic Conditions. *Journal of Hydrometeorology*, *17*(8), 2259–2274. https://doi.org/10.1175/JHM-D-15-0202.1

Behera, M. D., Borate, S. N., Panda, S. N., Behera, P. R., & Roy, P. S. (2012). Modelling and analyzing the watershed dynamics using Cellular Automata (CA)-Markov model - A geo-information based approach. *Journal of Earth System Science*, *121*(4), 1011–1024. https://doi.org/10.1007/s12040-012-0207-5

Bitew, M. M., Gebremichael, M., Ghebremichael, L. T., & Bayissa, Y. A. (2012). Evaluation of High-Resolution Satellite Rainfall Products through Streamflow Simulation in a Hydrological Modeling of a Small Mountainous Watershed in Ethiopia. *Journal of Hydrometeorology*, *13*(1), 338–350. https://doi.org/10.1175/2011JHM1292.1

Bosmans, J. H. C., van Beek, L. P. H., Sutanudjaja, E. H., & Bierkens, M. F. P. (2017). Hydrological impacts of global land cover change and human water use. *Hydrology and Earth System Sciences*, *21*(11), 5603–5626. https://doi.org/10.5194/hess-21-5603-2017

Brasil, J. B., Andrade, E. M. de, Palácio, H. A. de Q., Medeiros, P. H. A., & Santos, J. C. N. dos. (2018). Characteristics of precipitation and the process of interception in a seasonally dry tropical forest. *Journal of Hydrology: Regional Studies*, *19*(October), 307–317. https://doi.org/10.1016/j.ejrh.2018.10.006

Brunner, P., & Simmons, C. T. (2012). HydroGeoSphere: A Fully Integrated, Physically Based Hydrological Model. *Ground Water*, *50*(2), 170–176. https://doi.org/10.1111/j.1745-6584.2011.00882.x

Brunsdon, C., Fotheringham, A. S., & Charlton, M. E. (1996). Geographically Weighted Regression: A Method for Exploring Spatial Nonstationarity. *Geographical Analysis*, *28*(4).

Camici, S., Ciabatta, L., Massari, C., & Brocca, L. (2018). How reliable are satellite precipitation estimates for driving hydrological models: A verification study over the Mediterranean area. *Journal of Hydrology*, *563*(May), 950–961.

https://doi.org/10.1016/j.jhydrol.2018.06.067

Camporese, M., Paniconi, C., Putti, M., & Orlandini, S. (2010). Surface-subsurface flow modeling with path-based runoff routing, boundary condition-based coupling, and assimilation of multisource observation data. *Water Resources Research*, *46*(2). https://doi.org/10.1029/2008WR007536

Chao, L., Zhang, K., Li, Z., Zhu, Y., Wang, J., & Yu, Z. (2018). Geographically weighted regression based methods for merging satellite and gauge precipitation. *Journal of Hydrology*, *558*, 275–289. https://doi.org/10.1016/j.jhydrol.2018.01.042

Charlton, M., & Fotheringham, A. (2009). Geographically weighted regression: white paper. *White Paper*, 1–17. https://doi.org/10.1111/1467-9884.00145

Cleugh, H. A., Leuning, R., Mu, Q., & Running, S. W. (2007). Regional evaporation estimates from flux tower and MODIS satellite data. *Remote Sensing of Environment*, *106*(3), 285–304. https://doi.org/10.1016/j.rse.2006.07.007

De Bruin, H. A. R., & Lablans, W. N. (1998). Reference crop evapotranspiration determined with a modified Makkink equation. *Hydrological Processes*, *12*(7), 1053–1062. https://doi.org/10.1002/(SICI)1099-1085(19980615)12:7<1053::AID-HYP639>3.0.CO;2-E

de Bruin, H. A. R., Trigo, I. F., Bosveld, F. C., & Meirink, J. F. (2016). A Thermodynamically Based Model for Actual Evapotranspiration of an Extensive Grass Field Close to FAO Reference, Suitable for Remote Sensing Application. *Journal of Hydrometeorology*, *17*(5), 1373–1382. https://doi.org/10.1175/JHM-D-15-0006.1

De Bruin, H. A. R., Trigo, I. F., Jitan, M. A., Temesgen Enku, N., Van Der Tol, C., & Gieske, A. S. M. (2010). Reference crop evapotranspiration derived from geo-stationary satellite imagery: A case study for the Fogera flood plain, NW-Ethiopia and the Jordan Valley, Jordan. *Hydrology and Earth System Sciences*, *14*(11), 2219–2228. https://doi.org/10.5194/hess-14-2219-2010

Dinku, T., Ceccato, P., & Connor, S. J. (2011). Challenges of satellite rainfall estimation over mountainous and arid parts of east africa. *International Journal of Remote Sensing*, *32*(21), 5965–5979. https://doi.org/10.1080/01431161.2010.499381

Dinku, T., Chidzambwa, S., Ceccato, P., Connor, S. J., & Ropelewski, C. F. (2008). Validation of high-resolution satellite rainfall products over complex terrain. *International Journal of Remote Sensing*, *29*(14), 4097–4110. https://doi.org/10.1080/01431160701772526

Dinku, T., Funk, C., Peterson, P., Maidment, R., Tadesse, T., Gadain, H., & Ceccato, P. (2018). Validation of the CHIRPS satellite rainfall estimates over eastern Africa. *Quarterly Journal of the Royal Meteorological Society*, (April). https://doi.org/10.1002/qj.3244

Dinku, T., Hailemariam, K., Maidment, R., Tarnavsky, E., & Connor, S. (2014). Combined use of satellite estimates and rain gauge observations to generate high-quality historical rainfall time series over Ethiopia. *International Journal of Climatology*, *34*(7), 2489–2504. https://doi.org/10.1002/joc.3855

Dinku, T., Thomson, M. C., Cousin, R., del Corral, J., Ceccato, P., Hansen, J., & Connor, S. J. (2018). Enhancing National Climate Services (ENACTS) for development in Africa. *Climate and Development*, *10*(7), 664–672. https://doi.org/10.1080/17565529.2017.1405784

Distefano, T., & Kelly, S. (2017). Are we in deep water? Water scarcity and its limits to economic growth. *Ecological Economics*, *142*, 130–147. https://doi.org/10.1016/j.ecolecon.2017.06.019

dos Reis, J. B. C., Rennó, C. D., & Lopes, E. S. S. (2017). Validation of satellite rainfall products over a mountainouswatershed in a humid subtropical climate region of Brazil. *Remote Sensing*, *9*(12). https://doi.org/10.3390/rs9121240

Eastman, J. R. (2012). IDRISI Selva Manual, Version 17. Clark University.pp101, (January), 45.

El-Zehairy, A. A., Lubczynski, M. W., & Gurwin, J. (2018). مع(Modflow). *Hydrogeology Journal*, *26*(1), 109–132. https://doi.org/10.1007/s10040-017-1641-x

Fang, J., Du, J., Xu, W., Shi, P., Li, M., & Ming, X. (2013). Spatial downscaling of TRMM precipitation data based on the orographical effect and meteorological conditions in a mountainous area. *Advances in Water Resources*, *61*, 42–50. https://doi.org/10.1016/j.advwatres.2013.08.011

Feng, D., Zheng, Y., Mao, Y., Zhang, A., Wu, B., Li, J., … Wu, X. (2018a). An integrated hydrological modeling approach for detection and attribution of climatic and human impacts on coastal water resources. *Journal of Hydrology*, *557*, 305–320. https://doi.org/10.1016/j.jhydrol.2017.12.041

Feng, D., Zheng, Y., Mao, Y., Zhang, A., Wu, B., Li, J., … Wu, X. (2018b). An integrated hydrological modeling approach for detection and attribution of climatic and human impacts on coastal water resources. *Journal of Hydrology*, *557*(December), 305–320. https://doi.org/10.1016/j.jhydrol.2017.12.041

Fenta, A. A., Yasuda, H., Shimizu, K., Ibaraki, Y., Haregeweyn, N., Kawai, T., … Ebabu, K. (2018). Evaluation of satellite rainfall estimates over the Lake Tana basin at the source region of the Blue Nile River. *Atmospheric Research*, *212*(November 2017), 43–53. https://doi.org/10.1016/j.atmosres.2018.05.009

Fulton, J. W., Risser, D. W., Regan, R. S., Walker, R. J., Niswonger, R. G., Hoffman, S. A., & Markstrom, S. L. (2015). Water-budget and recharge-area simulations for Spring Creek and Nittany Creek basins and parts of the Spruce Creek basin, Centre and Huntingdon Counties, Pennsylvania, water years 2000–06. *U.S. Geological Survey Scientific Investigations Report 2015-5073*, 86. https://doi.org/10.3133/sir20155073

Funk, C., Peterson, P., Landsfeld, M., Pedreros, D., Verdin, J., Shukla, S., … Michaelsen, J. (2015). The climate hazards infrared precipitation with stations - A new environmental record for monitoring extremes. *Scientific Data*, *2*, 1–21. https://doi.org/10.1038/sdata.2015.66

García-Leoz, V., Villegas, J. C., Suescún, D., Flórez, C. P., Merino-Martín, L., Betancur, T., & León, J. D. (2018). Land cover effects on water balance partitioning in the Colombian Andes: improved water availability in early stages of natural vegetation recovery. *Regional Environmental Change*, *18*(4), 1117–1129. https://doi.org/10.1007/s10113-017-1249-7

Gashaw, T., Tulu, T., Argaw, M., & Worqlul, A. W. (2017). Evaluation and prediction of land use/land cover changes in the Andassa watershed, Blue Nile Basin, Ethiopia. *Environmental Systems Research*, *6*(1), 17. https://doi.org/10.1186/s40068-017-0094-5

Gebremicael, T. G., Mohamed, Y. A., Zaag, P. V., & Hagos, E. Y. (2017). *Temporal and spatial changes of rainfall and streamflow in the Upper Tekezē-Atbara river basin, Ethiopia*. *Hydrology and Earth System Sciences* (Vol. 21). https://doi.org/10.5194/hess-21-2127-2017

Gebreyohannes, T., De Smedt, F., Walraevens, K., Gebresilassie, S., Hussien, A., Hagos, M., … Gebrehiwot, K. (2017). Regional groundwater flow modeling of the Geba basin, northern Ethiopia. *Hydrogeology Journal*, *25*(3), 639–655. https://doi.org/10.1007/s10040-016-1522-8

Ghilain, N., Arboleda, A., & Gellens-Meulenberghs, F. (2011). Evapotranspiration modelling at large scale using near-real time MSG SEVIRI derived data. *Hydrology and Earth System Sciences*, *15*(3), 771–786. https://doi.org/10.5194/hess-15-771-2011

Ghosh, P., Mukhopadhyay, A., Chanda, A., Mondal, P., Akhand, A., Mukherjee, S., … Hazra, S. (2017). Application of Cellular automata and Markov-chain model in geospatial environmental modeling- A review. *Remote Sensing Applications: Society and*

Environment, *5*(April 2016), 64–77. https://doi.org/10.1016/j.rsase.2017.01.005
Gidey, E., Dikinya, O., Sebego, R., Segosebe, E., & Zenebe, A. (2017). Cellular automata and Markov Chain (CA_Markov) model-based predictions of future land use and land cover scenarios (2015–2033) in Raya, northern Ethiopia. *Modeling Earth Systems and Environment*, *3*(4), 1245–1262. https://doi.org/10.1007/s40808-017-0397-6
Girmay, E., Ayenew, T., Kebede, S., Alene, M., Wohnlich, S., & Wisotzky, F. (2015). Conceptual groundwater flow model of the Mekelle Paleozoic–Mesozoic sedimentary outlier and surroundings (northern Ethiopia) using environmental isotopes and dissolved ions. *Hydrogeology Journal*, *23*(4), 649–672. https://doi.org/10.1007/s10040-015-1243-4
Girmay, E. H. (2015). Litho – structural Controls on the Groundwater Flow System and Hydrogeochemical Setup of the Mekelle Outlier and Surrounding Areas , Nothern Ethiopia. *PhD Thesis*.
Graham, D., & Butts, M. (2005). Flexible, integrated watershed modelling with MIKE SHE. In Watershed Models, Eds. V.P. Singh & D.K. Frevert. *CRC Press*, 245–271. https://doi.org/10.1201/9781420037432.ch10
Grinblat, Y., Kidron, G. J., Karnieli, A., & Benenson, I. (2015). Simulating land-use degradation in West Africa with the ALADYN model. *Journal of Arid Environments*, *112*(PA), 52–63. https://doi.org/10.1016/j.jaridenv.2014.05.019
Gyamfi, C., Ndambuki, J. M., & Salim, R. W. (2016). Hydrological responses to land use/cover changes in the Olifants Basin, South Africa. *Water*, *8*(12). https://doi.org/10.3390/w8120588
Habib, E., Haile, A. T., Sazib, N., Zhang, Y., & Rientjes, T. (2014). Effect of bias correction of satellite-rainfall estimates on runoff simulations at the source of the Upper Blue Nile. *Remote Sensing*, *6*(7), 6688–6708. https://doi.org/10.3390/rs6076688
Habib, E., Larson, B. F., & Graschel, J. (2009). Validation of NEXRAD multisensor precipitation estimates using an experimental dense rain gauge network in south Louisiana. *Journal of Hydrology*, *373*(3–4), 463–478. https://doi.org/10.1016/j.jhydrol.2009.05.010
Haddeland, I., Heinke, J., Biemans, H., Eisner, S., Flörke, M., Hanasaki, N., … Wisser, D. (2014). Global water resources affected by human interventions and climate change. *Proceedings of the National Academy of Sciences*, *111*(9), 3251–3256. https://doi.org/10.1073/pnas.1222475110
Haile, A. T., Habib, E., & Rientjes, T. (2013). Evaluation of the climate prediction center (CPC) morphing technique (CMORPH) rainfall product on hourly time scales over the source of the Blue Nile River. *Hydrological Processes*, *27*(12), 1829–1839. https://doi.org/10.1002/hyp.9330
Haregeweyn, N., Tesfaye, S., Tsunekawa, A., Tsubo, M., Meshesha, D. T., Adgo, E., & Elias, A. (2015). Dynamics of land use and land cover and its effects on hydrologic responses: case study of the Gilgel Tekeze catchment in the highlands of Northern Ethiopia. *Environmental Monitoring and Assessment*, *187*(1). https://doi.org/10.1007/s10661-014-4090-1
Hargreaves, G. H., & Samani, Z. . (1985). Reference Crop Evapotranspiration from Temperature. *Applied Engineering in Agriculture*, *1*(2), 96–99. https://doi.org/10.13031/2013.26773
Hassan, S. M. T., Lubczynski, M. W., Niswonger, R. G., & Su, Z. (2014). *Surface-groundwater interactions in hard rocks in Sardon Catchment of western Spain: An integrated modeling approach*. *Journal of Hydrology* (Vol. 517). Elsevier B.V. https://doi.org/10.1016/j.jhydrol.2014.05.026
Hoyer, R., & Chang, H. (2014). Development of Future Land Cover Change Scenarios in the Metropolitan Fringe, Oregon, U.S., with Stakeholder Involvement. *Land*, *3*(1), 322–341.

https://doi.org/10.3390/land3010322

Hu, Q., Yang, H., Meng, X., Wang, Y., & Deng, P. (2015). Satellite and gauge rainfall merging using geographically weighted regression. *Remote Sensing and GIS for Hydrology and Water Resources*, *368*(August 2014), 132–137. https://doi.org/10.5194/piahs-368-132-2015

Huntington, J. L., & Niswonger, R. G. (2012). Role of surface-water and groundwater interactions on projected summertime streamflow in snow dominated regions: An integrated modeling approach. *Water Resources Research*, *48*(11), 1–20. https://doi.org/10.1029/2012WR012319

Hyandye, C., & Martz, L. W. (2017). A Markovian and cellular automata land-use change predictive model of the Usangu Catchment. *International Journal of Remote Sensing*, *38*(1), 64–81. https://doi.org/10.1080/01431161.2016.1259675

Jinno, K., Tsutsumi, A., Alkaeed, O., Saita, S., & Berndtsson, R. (2009). Effects of land-use change on groundwater recharge model parameters. *Hydrological Sciences Journal*, *54*(2), 300–315. https://doi.org/10.1623/hysj.54.2.300

Joo, J., Tian, Y., Zheng, C., Zheng, Y., Sun, Z., Zhang, A., & Chang, H. (2018). An Integrated Modeling Approach to Study the Surface Water-Groundwater Interactions and Influence of Temporal Damping Effects on the Hydrological Cycle in the Miho Catchment in South Korea. *Water*, *10*(11), 1529. https://doi.org/10.3390/w10111529

Kahle, D. M. E. and S. C. (2012). Simulation of groundwater and surface-water resources and evaluation of water-management alternatives for the Chamokane Creek basin, Stevens County, Washington Scientific Investigations Report 2012-5224. Retrieved from https://pubs.er.usgs.gov/publication/sir20125224

Karimi, P., & Bastiaanssen, W. G. M. (2015). Spatial evapotranspiration, rainfall and land use data in water accounting - Part 1: Review of the accuracy of the remote sensing data. *Hydrology and Earth System Sciences*, *19*(1), 507–532. https://doi.org/10.5194/hess-19-507-2015

Kebede, S., Hailu, A., Crane, E., Ó Dochartaigh, B.É and Bellwood-Howard, I. (2018). Africa Groundwater Atlas: Hydrogeology of Ethiopia. British Geological Survey. Accessed [September 6, 2018]. Retrieved from http://earthwise.bgs.ac.uk/index.php/Hydrogeology_of_Ethiopia#Soil

Kebede, S. (2013). *Groundwater in Ethiopia: Features, numbers and opportunities*. *Springer Hydrogeology*. https://doi.org/10.1007/978-3-642-30391-3

Kebede, S., Travi, Y., Alemayehu, T., & Ayenew, T. (2006). Groundwater recharge, circulation and geochemical evolution in the source region of the Blue Nile River, Ethiopia. *Applied Geochemistry*, *20*(9), 1658–1676. https://doi.org/10.1016/j.apgeochem.2005.04.016

Keshtkar, H., & Voigt, W. (2016). A spatiotemporal analysis of landscape change using an integrated Markov chain and cellular automata models. *Modeling Earth Systems and Environment*, *2*(1), 10. https://doi.org/10.1007/s40808-015-0068-4

Kidd, C. (2001). Satellite rainfall climatology: A review. *International Journal of Climatology*, *21*(9), 1041–1066. https://doi.org/10.1002/joc.635

Kim, J. H., & Jackson, R. B. (2012). A Global Analysis of Groundwater Recharge for Vegetation, Climate, and Soils. *Vadose Zone Journal*, *11*(1), 0. https://doi.org/10.2136/vzj2011.0021RA

Kim, J., & Hogue, T. S. (2008). Evaluation of a MODIS-Based Potential Evapotranspiration Product at the Point Scale. *Journal of Hydrometeorology*, *9*(3), 444–460. https://doi.org/10.1175/2007JHM902.1

Kimani, M. W., Hoedjes, J. C. B., & Su, Z. (2017). An assessment of satellite-derived rainfall products relative to ground observations over East Africa. *Remote Sensing*, *9*(5).

https://doi.org/10.3390/rs9050430

Kindu, M., Schneider, T., Döllerer, M., Teketay, D., & Knoke, T. (2018). Scenario modelling of land use/land cover changes in Munessa-Shashemene landscape of the Ethiopian highlands. *Science of the Total Environment*, *622–623*, 534–546. https://doi.org/10.1016/j.scitotenv.2017.11.338

Kumar, N., Kumar, S., Vikram, S., Singh, G., & Dzwairo, B. (2018). Investigation of impacts of land use / land cover change on water availability of Tons River Basin , Madhya Pradesh , India. *Modeling Earth Systems and Environment*, *0*(0), 0. https://doi.org/10.1007/s40808-018-0425-1

Lang, D., Zheng, J., Shi, J., Liao, F., Ma, X., Wang, W., … Zhang, M. (2017). A comparative study of potential evapotranspiration estimation by eight methods with FAO Penman–Monteith method in southwestern China. *Water (Switzerland)*, *9*(10). https://doi.org/10.3390/w9100734

Lekula, M., Lubczynski, M. W., & Shemang, E. M. (2018). Hydrogeological conceptual model of large and complex sedimentary aquifer systems – Central Kalahari Basin. *Physics and Chemistry of the Earth*, (July), 0–1. https://doi.org/10.1016/j.pce.2018.05.006

Lekula, M., Lubczynski, M. W., Shemang, E. M., & Verhoef, W. (2018). Validation of satellite-based rainfall in Kalahari. *Physics and Chemistry of the Earth*, *105*(February), 84–97. https://doi.org/10.1016/j.pce.2018.02.010

Li, X., Xiao, Q., Niu, J., Dymond, S., van Doorn, N. S., Yu, X., … Li, J. (2016). Process-based rainfall interception by small trees in Northern China: The effect of rainfall traits and crown structure characteristics. *Agricultural and Forest Meteorology*, *218–219*, 65–73. https://doi.org/10.1016/j.agrformet.2015.11.017

Liang, X. (2003). A new parameterization for surface and groundwater interactions and its impact on water budgets with the variable infiltration capacity (VIC) land surface model. *Journal of Geophysical Research*, *108*(D16), 8613. https://doi.org/10.1029/2002JD003090

Liu, Y. B., Smedt, F. De, Hoffmann, L., & Pfister, L. (2004). Assessing land use impacts on flood processes in complex terrain. *Environmental Modeling and Assessment 9:*, *9*, 227–235.

LSA LISA Team. (2016). Algorithm Theoretical Basis Document for Reference Evapotranspiration (DMETREF): ATBD_DMETREF, Product LSA-303. SAF/LAND/ IPMA/ATBD_METREF/1.1. Retrieved from https://landsaf.ipma.pt/en/products/evapotranspiration/

Lu, B., Charlton, M., Harris, P., & Fotheringham, A. S. (2014). Geographically weighted regression with a non-Euclidean distance metric: A case study using hedonic house price data. *International Journal of Geographical Information Science*, *28*(4), 660–681. https://doi.org/10.1080/13658816.2013.865739

Lubczynski, M. W. (2006). Groundwater fluxes in arid and semi-arid environments.pdf. *Groundwater and Ecosystems*, 225–236.

Lubczynski, M. W., & Gurwin, J. (2005). Integration of various data sources for transient groundwater modeling with spatio-temporally variable fluxes - Sardon study case, Spain. *Journal of Hydrology*, *306*(1–4), 71–96. https://doi.org/10.1016/j.jhydrol.2004.08.038

Luetkemeier, R., Stein, L., Drees, L., Müller, H., & Liehr, S. (2018). Uncertainty of rainfall products: Impact on modelling household nutrition from rain-fed agriculture in Southern Africa. *Water (Switzerland)*, *10*(4), 1–23. https://doi.org/10.3390/w10040499

Lv, A., & Zhou, L. (2016). A rainfall model based on a Geographically Weighted Regression algorithm for rainfall estimations over the arid Qaidam Basin in China. *Remote Sensing*, *8*(4). https://doi.org/10.3390/rs8040311

Ma, Y., Hong, Y., Chen, Y., Yang, Y., Tang, G., Yao, Y., … Liu, R. (2018). Performance of Optimally

Merged Multisatellite Precipitation Products Using the Dynamic Bayesian Model Averaging Scheme Over the Tibetan Plateau. *Journal of Geophysical Research: Atmospheres*, *123*(2), 814–834. https://doi.org/10.1002/2017JD026648

Maathuis, B., Mannaerts, C., Retsios, B., Bie, K. De, & Nieuwenhuis, W. (2018a). Water and food security-Ethiopia toolbox.Faculty of Geo-information Science & Earth Observation (ITC). University of Twente, Enschede, The Netherlands.ftp://ftp.itc.nl/pub/52n/WFS-EthiopiaTB2/.

Maathuis, B., Mannaerts, C., Retsios, B., Bie, K. De, & Nieuwenhuis, W. (2018b). WATER AND FOOD SECURITY-ETHIOPIA TOOLBOX, (November).

Maeda, E. E., Wiberg, D. A., & Pellikka, P. K. E. (2011). Estimating reference evapotranspiration using remote sensing and empirical models in a region with limited ground data availability in Kenya. *Applied Geography*, *31*(1), 251–258. https://doi.org/10.1016/j.apgeog.2010.05.011

Mao, D., & Cherkauer, K. A. (2009). Impacts of land-use change on hydrologic responses in the Great Lakes region. *Journal of Hydrology*, *374*(1–2), 71–82. https://doi.org/10.1016/j.jhydrol.2009.06.016

Markstrom, S. L., Niswonger, R. G., Regan, R. S., Prudic, D. E., & Barlow, P. M. (2008). GSFLOW - Coupled Ground-Water and Surface-Water Flow Model Based on the Integration of the Precipitation-Runoff Modeling System (PRMS) and the Modular Ground-Water Flow Model (MODFLOW-2005). *U.S. Geological Survey. Techniques and Methods 6-D1*, (Techniques and Methods 6-D1), 254. https://doi.org/10.1109/CarpathianCC.2015.7145042

Mateus, C., Tullos, D. D., & Surfleet, C. G. (2015). Hydrologic sensitivity to climate and land use changes in the Santiam River Basin, Oregon. *Journal of the American Water Resources Association*, *51*(2), 400–420. https://doi.org/10.1111/jawr.12256

McMahon, T. A., Peel, M. C., Lowe, L., Srikanthan, R., & McVicar, T. R. (2013). Estimating actual, potential, reference crop and pan evaporation using standard meteorological data: A pragmatic synthesis. *Hydrology and Earth System Sciences*, *17*(4), 1331–1363. https://doi.org/10.5194/hess-17-1331-2013

Melesse, A. M., & Abtew, W. (2015). Landscape Dynamics, Soils and Hydrological Processes in Varied Climates. *Landscape Dynamics, Soils and Hydrological Processes in Varied Climates*, 1–839. https://doi.org/10.1007/978-3-319-18787-7

Melesse, A. M., Abtew, W., & Setegn, S. G. (2013). *Nile River Basin: Ecohydrological challenges, climate change and hydropolitics*. *Nile River Basin: Ecohydrological Challenges, Climate Change and Hydropolitics*. https://doi.org/10.1007/978-3-319-02720-3

Mohan, C., Western, A. W., Wei, Y., & Saft, M. (2018). Predicting groundwater recharge for varying land cover and climate conditions-a global meta-study. *Hydrology and Earth System Sciences*, *22*(5), 2689–2703. https://doi.org/10.5194/hess-22-2689-2018

Moral, F. J., Rebollo, F. J., Paniagua, L. L., GarcÃ-a-MartÃ-n, A., & Honorio, F. (2016). Spatial distribution and comparison of aridity indices in Extremadura, southwestern Spain. *Theoretical and Applied Climatology*, *126*(3–4), 801–814. https://doi.org/10.1007/s00704-015-1615-7

Nash, E., & Sutcliffe, V. (1970). River flow forecasting through conceptual models: Part 1. A discussion of principles. *Journal of Hydrology*, *10*, 282–290. https://doi.org/10.1016/0022-1694(70)90255-6

Ndou, N. N., Palamuleni, L. G., & Ramoelo, A. (2017). Modelling depth to groundwater level using SEBAL-based dry season potential evapotranspiration in the upper Molopo River Catchment, South Africa. *Egyptian Journal of Remote Sensing and Space Science*, *21*(3), 237–248. https://doi.org/10.1016/j.ejrs.2017.08.003

Nerini, D., Zulkafli, Z., Wang, L.-P., Onof, C., Buytaert, W., Lavado-Casimiro, W., & Guyot, J.-L. (2015). A Comparative Analysis of TRMM–Rain Gauge Data Merging Techniques at the Daily Time Scale for Distributed Rainfall–Runoff Modeling Applications. *Journal of Hydrometeorology*, *16*(5), 2153–2168. https://doi.org/10.1175/JHM-D-14-0197.1

Niu, G. Y., Troch, P. A., Paniconi, C., Scott, R. L., Durcik, M., Zeng, X., … Pelletier, J. (2014). An integrated modelling framework of catchment-scale ecohydrological processes: 2. The role of water subsidy by overland flow on vegetation dynamics in a semi-arid catchment. *Ecohydrology*, *7*(2), 815–827. https://doi.org/10.1002/eco.1405

Oudin, L., Moulin, L., Bendjoudi, H., & Ribstein, P. (2010). Estimating potential evapotranspiration without continuous daily data: possible errors and impact on water balance simulations. *Hydrological Sciences Journal*, *55*(2), 209–222. https://doi.org/10.1080/02626660903546118

Öztürk, M., Copty, N. K., & Saysel, A. K. (2013). Modeling the impact of land use change on the hydrology of a rural watershed. *Journal of Hydrology*, *497*, 97–109. https://doi.org/10.1016/j.jhydrol.2013.05.022

Panday, S., Langevin, C. D., Niswonger, R. G., Ibaraki, M., & Hughes, J. D. (2013). MODFLOW-USG: An Unstructured Grid Version of MODFLOW for Simulating Groundwater Flow and Tightly Coupled Processes Using a Control Volume Finite-Difference Formulation. *U.S. Geological Survey, Reston, Virginia*. Retrieved from http://water.usgs.gov/ogw/mfusg

Philip, S., Kew, S. F., van Oldenborgh, G. J., Otto, F., O'Keefe, S., Haustein, K., … Cullen, H. (2018). Attribution analysis of the Ethiopian drought of 2015. *Journal of Climate*, *31*(6), 2465–2486. https://doi.org/10.1175/JCLI-D-17-0274.1

Priestley, C. H. B., & Taylor, R. J. (1972). On the Assessment of Surface Heat Flux and Evaporation Using Large-Scale Parameters. *Mon. Weather Rev*, *100*, 81–92. https://doi.org/10.5021/ad.2014.26.5.655

Pulido-Velazquez, M., Peña-Haro, S., García-Prats, A., Mocholi-Almudever, A. F., Henriquez-Dole, L., Macian-Sorribes, H., & Lopez-Nicolas, A. (2015). Integrated assessment of the impact of climate and land use changes on groundwater quantity and quality in the Mancha Oriental system (Spain). *Hydrol. Earth Syst. Sci*, 1677–1693. https://doi.org/10.5194/hess-19-1677-2015

Rahmawati, N., & Lubczynski, M. W. (2017). Validation of satellite daily rainfall estimates in complex terrain of Bali Island, Indonesia. *Theoretical and Applied Climatology*, 1–20. https://doi.org/10.1007/s00704-017-2290-7

Retalis, A., Tymvios, F., Katsanos, D., & Michaelides, S. (2017). Downscaling CHIRPS precipitation data: an artificial neural network modelling approach. *International Journal of Remote Sensing*, *38*(13), 3943–3959. https://doi.org/10.1080/01431161.2017.1312031

Rivest, M., Marcotte, D., & Pasquier, P. (2008). Hydraulic head field estimation using kriging with an external drift: A way to consider conceptual model information. *Journal of Hydrology*, *361*(3–4), 349–361. https://doi.org/10.1016/j.jhydrol.2008.08.006

Rost, S., Gerten, D., Bondeau, A., Lucht, W., Rohwer, J., & Schaphoff, S. (2008). Agricultural green and blue water consumption and its influence on the global water system. *Water Resources Research*, *44*(9), 1–17. https://doi.org/10.1029/2007WR006331

Sajikumar, N., & Remya, R. S. (2015). Impact of land cover and land use change on runoff characteristics. *Journal of Environmental Management*, *161*, 460–468. https://doi.org/10.1016/j.jenvman.2014.12.041

Samie, A., Deng, X., Jia, S., & Chen, D. (2017). Scenario-based simulation on dynamics of land-use-land-cover change in Punjab province, Pakistan. *Sustainability*, *9*(8).

https://doi.org/10.3390/su9081285
Schaldach, R., Alcamo, J., Koch, J., Kölking, C., Lapola, D. M., Schüngel, J., & Priess, J. A. (2011). An integrated approach to modelling land-use change on continental and global scales. *Environmental Modelling and Software*, *26*(8), 1041–1051. https://doi.org/10.1016/j.envsoft.2011.02.013
Searcy, J. K., & Hardison, C. H. (1960). *Double-Mass Curves. Manual of Hydrology:Part 1. General Surface-Water Techniques*. *U.S Geological Survey Water Supply Paper 1541B*. https://doi.org/http://udspace.udel.edu/handle/19716/1592
Sebben, M. L., Werner, A. D., Liggett, J. E., Partington, D., & Simmons, C. T. (2013). On the testing of fully integrated surface-subsurface hydrological models. *Hydrological Processes*, *27*(8), 1276–1285. https://doi.org/10.1002/hyp.9630
Sembroni, A., Molin, P., Dramis, F., & Abebe, B. (2017). Geology of the tekeze river basin (Northern Ethiopia). *Journal of Maps*, *13*(2), 621–631. https://doi.org/10.1080/17445647.2017.1351907
Setyorini, A., Khare, D., & Pingale, S. M. (2017). Simulating the impact of land use/land cover change and climate variability on watershed hydrology in the Upper Brantas basin, Indonesia. *Applied Geomatics*, *9*(3), 191–204. https://doi.org/10.1007/s12518-017-0193-z
Seyyedi, H., Anagnostou, E. N., Beighley, E., & McCollum, J. (2014). Satellite-driven downscaling of global reanalysis precipitation products for hydrological applications. *Hydrology and Earth System Sciences*, *18*(12), 5077–5091. https://doi.org/10.5194/hess-18-5077-2014
Shaw, S. B., & Riha, S. J. (2011). Assessing temperature-based PET equations under a changing climate in temperate, deciduous forests. *Hydrological Processes*, *25*(9), 1466–1478. https://doi.org/10.1002/hyp.7913
Sheffield, J., Wood, E. F., & Roderick, M. L. (2012). Little change in global drought over the past 60 years. *Nature*, *491*(7424), 435–438. https://doi.org/10.1038/nature11575
Song, X., Zhang, J., Zhan, C., Xuan, Y., Ye, M., & Xu, C. (2015). Global sensitivity analysis in hydrological modeling: Review of concepts, methods, theoretical framework, and applications. *Journal of Hydrology*, *523*(225), 739–757. https://doi.org/10.1016/j.jhydrol.2015.02.013
Sridhar, V., Billah, M. M., & Hildreth, J. W. (2018). Coupled Surface and Groundwater Hydrological Modeling in a Changing Climate. *Groundwater*, *56*(4), 618–635. https://doi.org/10.1111/gwat.12610
Takahashi, S., Nakajima, R., Miyoshi, T., Takaya, Y., Yoshioka, T., Hariyama, T., … Takamasu, K. (2004). Nano-defects inspection of semiconductor wafer using evanescent wave. *VDI Berichte*, (1844). https://doi.org/10.1007/3-540-32202-7
Taye, G., Poesen, J., Vanwesemael, B., Vanmaercke, M., & Teka, D. (2014). Effectiveness of soil and water conservation structures in reducing runoff and soil loss for different land use and slope gradients : Case study from northern Ethiopia. *Geophysical Research Abstracts*, *16*, 5452.
Teka, K., Van Rompaey, A., & Poesen, J. (2013). Assessing the role of policies on land use change and agricultural development since 1960s in northern Ethiopia. *Land Use Policy*, *30*(1), 944–951. https://doi.org/10.1016/j.landusepol.2012.07.005
Teklay, A., Dile, Y. T., Setegn, S. G., Demissie, S. S., & Asfaw, D. H. (2019). Evaluation of static and dynamic land use data for watershed hydrologic process simulation: A case study in Gummara watershed, Ethiopia. *Catena*, *172*(August 2018), 65–75. https://doi.org/10.1016/j.catena.2018.08.013
Tesfagiorgis, K., Gebreyohannes, T., De Smedt, F., Moeyersons, J., Hagos, M., Nyssen, J., &

Deckers, J. (2011). Evaluation of groundwater resources in the Geba basin, Ethiopia. *Bulletin of Engineering Geology and the Environment*, *70*(3), 461–466. https://doi.org/10.1007/s10064-010-0338-3

Thiemig, V., Rojas, R., Zambrano-Bigiarini, M., & De Roo, A. (2013). Hydrological evaluation of satellite-based rainfall estimates over the Volta and Baro-Akobo Basin. *Journal of Hydrology*, *499*, 324–338. https://doi.org/10.1016/j.jhydrol.2013.07.012

Tian, Y., Zheng, Y., Han, F., Zheng, C., & Li, X. (2018). A comprehensive graphical modeling platform designed for integrated hydrological simulation. *Environmental Modelling and Software*, *108*(December 2017), 154–173. https://doi.org/10.1016/j.envsoft.2018.08.011

Tian, Y., Zheng, Y., Wu, B., Wu, X., Liu, J., & Zheng, C. (2015). Modeling surface water-groundwater interaction in arid and semi-arid regions with intensive agriculture. *Environmental Modelling and Software*, *63*, 170–184. https://doi.org/10.1016/j.envsoft.2014.10.011

Toté, C., Patricio, D., Boogaard, H., van der Wijngaart, R., Tarnavsky, E., & Funk, C. (2015). Evaluation of satellite rainfall estimates for drought and flood monitoring in Mozambique. *Remote Sensing*, *7*(2), 1758–1776. https://doi.org/10.3390/rs70201758

Trigo, I. F., de Bruin, H., Beyrich, F., Bosveld, F. C., Gavilán, P., Groh, J., & López-Urrea, R. (2018). Validation of reference evapotranspiration from Meteosat Second Generation (MSG) observations. *Agricultural and Forest Meteorology*, *259*(September 2017), 271–285. https://doi.org/10.1016/j.agrformet.2018.05.008

Vanderkwaak, J. E., & Loague, K. (2001). Hydrologic-response simulations for the R-5 catchment with a comprehensive physics-based model. *Water Resources Research*, *37*(4), 999–1013.

Wagner, P. D., Kumar, S., & Schneider, K. (2013). An assessment of land use change impacts on the water resources of the Mula and Mutha Rivers catchment upstream of Pune, India. *Hydrology and Earth System Sciences*, *17*(6), 2233–2246. https://doi.org/10.5194/hess-17-2233-2013

Welde, K., & Gebremariam, B. (2017). Effect of land use land cover dynamics on hydrological response of watershed: Case study of Tekeze Dam watershed, northern Ethiopia. *International Soil and Water Conservation Research*, *5*(1), 1–16. https://doi.org/10.1016/j.iswcr.2017.03.002

Weng, Q. (2002). Land use change analysis in the Zhujiang Delta of China using satellite remote sensing, GIS and stochastic modelling. *Journal of Environmental Management*, *64*(3), 273–284. https://doi.org/10.1006/jema.2001.0509

Woldesenbet, T. A., Elagib, N. A., Ribbe, L., & Heinrich, J. (2017). Hydrological responses to land use/cover changes in the source region of the Upper Blue Nile Basin, Ethiopia. *Science of the Total Environment*, *575*, 724–741. https://doi.org/10.1016/j.scitotenv.2016.09.124

Worqlul, A. W., Ayana, E. K., Maathuis, B. H. P., MacAlister, C., Philpot, W. D., Osorio Leyton, J. M., & Steenhuis, T. S. (2018). Performance of bias corrected MPEG rainfall estimate for rainfall-runoff simulation in the upper Blue Nile Basin, Ethiopia. *Journal of Hydrology*, *556*, 1182–1191. https://doi.org/10.1016/j.jhydrol.2017.01.058

Worqlul, A. W., Jeong, J., Dile, Y. T., Osorio, J., Schmitter, P., Gerik, T., … Clark, N. (2017). Assessing potential land suitable for surface irrigation using groundwater in Ethiopia. *Applied Geography*, *85*, 1–13. https://doi.org/10.1016/j.apgeog.2017.05.010

Worqlul, A. W., Maathuis, B., Adem, A. A., Demissie, S. S., Langan, S., & Steenhuis, T. S. (2014). Comparison of rainfall estimations by TRMM 3B42, MPEG and CFSR with ground-observed data for the Lake Tana basin in Ethiopia. *Hydrology and Earth System Sciences*, *18*(12), 4871–4881. https://doi.org/10.5194/hess-18-4871-2014

Wu, B., Zheng, Y., Tian, Y., Wu, X., Yao, Y., Han, F., … Zheng, C. (2014). Systematic assessment of the uncertainty in integrated surface water-groundwater modeling based on the probabilistic collocation method. *Water Resources Research*, *50*(7), 5848–5865. https://doi.org/10.1002/2014WR015366

Wu, B., Zheng, Y., Wu, X., Tian, Y., Han, F., Liu, J., & Zheng, C. (2015). Optimizing water resources management in large river basins with integrated surface water-groundwater modeling: A surrogate-based approach. *Water Resources Research*, (51), 5974–5997. https://doi.org/10.1002/2015WR017408.Received

Xu, C. Y., & Singh, V. P. (2000). Evaluation and generalization of radiation-based methods for calculationg evaporation. *Hydrological Processes*, *14*(January 1999), 339–349.

Xu, C. Y., & Singh, V. P. (2004). Review on regional water resources assessment models under stationary and changing climate. *Water Resources Management*, *18*(6), 591–612. https://doi.org/10.1007/s11269-004-9130-0

Yeh, P. J. F., & Eltahir, E. A. B. (2005). Representation of water table dynamics in a land surface scheme. Part I: Model development. *Journal of Climate*, *18*(12), 1861–1880. https://doi.org/10.1175/JCLI3330.1

Yihdego, B. Y., & Khalil, A. (2017). Economic and Environmental Management of Water Resources: Perspective of Groundwater. *Global Journal of HUMAN-SOCIAL SCIENCE: B Geography, Geo-Sciences, Environmental Science & Disaster Management*, *17*(2).

Zambrano-Bigiarini, M., Nauditt, A., Birkel, C., Verbist, K., & Ribbe, L. (2017). Temporal and spatial evaluation of satellite-based rainfall estimates across the complex topographical and climatic gradients of Chile. *Hydrology and Earth System Sciences*, *21*(2), 1295–1320. https://doi.org/10.5194/hess-21-1295-2017

Zhang, Z., Gong, Y., & Wang, Z. (2018). Accessible remote sensing data based reference evapotranspiration estimation modelling. *Agricultural Water Management*, *210*(July), 59–69. https://doi.org/10.1016/j.agwat.2018.07.039

Zhen, L., Deng, X., Wei, Y., Jiang, Q., Lin, Y., Helming, K., … Hu, J. (2014). Future land use and food security scenarios for the Guyuan district of remote western China. *IForest*, *7*(7), 372–384. https://doi.org/10.3832/ifor1170-007

Zhou, Q., Wang, W., Pang, Y., Zhou, Z. yong, & Luo, H. ping. (2015). Temporal and spatial distribution characteristics of water resources in Guangdong Province based on a cloud model. *Water Science and Engineering*, *8*(4), 263–272. https://doi.org/10.1016/j.wse.2015.09.001

Zhou, Y., Qu, J., Wu, J., Liu, F., & Sources, A. D. (2015). Quantitatively Analyzed Vegetation Coverage and Its Dynamic Changes of Mulan County in Heilongjiang Province Based on RS and GIS. *International Conference on Industrial Electronics and Applications*, 519–522.

Zomlot, Z., Verbeiren, B., Huysmans, M., & Batelaan, O. (2017). Trajectory analysis of land use and land cover maps to improve spatial–temporal patterns, and impact assessment on groundwater recharge. *Journal of Hydrology*, *554*, 558–569. https://doi.org/10.1016/j.jhydrol.2017.09.032

Zwartendijk, B. (2015). Land cover effects on infiltration and preferential flow pathways in the high rainfall zone of Madagascar. *Geophysical Research Abstracts*, *17*(123456734), 2015–11840.